



**MARTHA CHRISTINE
MEDEIROS
GUERREIRO**

**MODELAÇÃO MORFODINÂMICA DA RIBEIRA DE
ALJEZUR**

**MORPHODYNAMIC MODELING OF THE ALJEZUR
STREAM**



**MARTHA CHRISTINE
MEDEIROS
GUERREIRO**

**MODELAÇÃO MORFODINÂMICA DA RIBEIRA DE
ALJEZUR**

**MORPHODYNAMIC MODELING OF THE ALJEZUR
STREAM**

Dissertação apresentada à Universidade de Aveiro para cumprimento dos requisitos necessários à obtenção do grau de Mestre em Ciências do Mar e Zonas Costeiras, realizada sob a orientação científica do Doutor André Bustorff Fortunato, Investigador Principal do Núcleo de Estuários e Zonas Costeiras do Laboratório Nacional de Engenharia Civil e do Professor Auxiliar João Miguel Dias do Departamento de Física da Universidade de Aveiro.

Este trabalho foi desenvolvido no âmbito do projecto MADyCOS (PTDC/ECM/66484/2006) com o apoio financeiro da Fundação para a Ciência e a Tecnologia – FCT e do Laboratório Nacional de Engenharia Civil.

o júri

presidente

Prof. Doutora Filomena Maria Cardoso Pedrosa Ferreira Martins
Professora Associada do Departamento de Ambiente e Ordenamento da Universidade de Aveiro

Doutora Anabela Pacheco de Oliveira
Investigadora Principal do Departamento de Hidráulica e Ambiente do Laboratório Nacional de Engenharia Civil (LNEC)

Doutor André Bustorff Fortunato
Investigador Principal do Departamento de Hidráulica e Ambiente do Laboratório Nacional de Engenharia Civil (LNEC)

Prof. Doutor João Miguel Sequeira Silva Dias
Professor Auxiliar do Departamento de Física da Universidade de Aveiro

agradecimentos

Este trabalho seria impensável realizá-lo sem o apoio de várias pessoas e entidades, às quais gostaria de agradecer.

Aos meus orientadores, Doutor André Bustorff Fortunato por toda a motivação, paciência e empenho transmitidos em todas as etapas deste trabalho, e Professor João Miguel Dias, pelas sugestões e disponibilidade demonstradas.

À Doutora Anabela Oliveira, por todo o apoio e motivação sempre demonstrados em todas as conversas, com especial destaque às “Brain storming” durante o café da manhã.

A todas as pessoas que participaram no projecto MADyCOS e tornaram possível a realização deste trabalho.

Ao LNEC – Laboratório Nacional de Engenharia Civil, por todas as condições de trabalho disponibilizadas.

Ao Professor Óscar Ferreira, pela disponibilização dos dados de batimetria da Praia da Amoreira, através do projecto BAYBEACH.

À Professora Conceição Freitas, pela disponibilização dos dados atmosféricos e condições marítimas da bóia de Sines, através do projecto DETI.

A todos que disponibilizarão as várias fotos da praia da Amoreira, em especial à Ana Silva.

A todos que contribuíram para o continuo desenvolvimento do MORSYS2D, em especial ao Doutor Xavier Bertin.

À equipa do modelo ELCIRC e SWAN, pela disponibilização dos códigos e software dos modelos.

Aos meus colegas Alberto Azevedo, Marta Rodrigues, Lúcia Pinto e Nicolas Bruneau por toda a disponibilidade sempre demonstrada para construir ideias.

À Alda Leão, pela sua persistência a resolver qualquer tipo de problema.

Aos meus amigos que me fazem sorrir em tantos momentos: Carina, Carlos, Francisco, Filipa, Mónica, Sara, Miguel e Carolina.

Um especial agradecimento à minha família que sempre me apoia em todo o meu percurso.

palavras-chave

Modelação morfodinâmica, embocaduras, ribeira de Aljezur.

resumo

A morfologia de embocaduras é muito dinâmica, devido à acção combinada das ondas, marés e caudais fluviais. As alterações morfológicas são particularmente relevantes em embocaduras pouco profundas e de pequenas dimensões, dado que ligeiras alterações na batimetria podem conduzir a um efeito dramático na propagação e distorção da maré. Ocasionalmente, estas dinâmicas complexas podem levar ao fecho da embocadura e consequentemente à deterioração da qualidade da água a montante. Os modelos numéricos morfodinâmicos constituem ferramentas atractivas para o estudo destas alterações morfológicas, embora a sua aplicação seja ainda demorada e necessite de um conhecimento profundo sobre os processos relevantes. Este estudo visa analisar a morfodinâmica da embocadura de um sistema costeiro de pequenas dimensões e profundidades (ribeira de Aljezur), através da implementação, validação e exploração do sistema de modelação morfodinâmico MORSYS2D. A ribeira de Aljezur está localizada na costa sudoeste de Portugal e está sujeita às ondas e ventos do Atlântico Norte e às marés ao longo da plataforma Ibérica. A ribeira tem cerca de 36 km de comprimento, com profundidades entre 1-3 m e uma largura entre 10-40 m. Cinco campanhas de campo foram realizadas entre 2008-2010, de forma a adquirir dados de batimetria, níveis de água, ondas e correntes, tanto no estuário como na praia adjacente, para a compreensão da dinâmica da ribeira e para a aplicação, calibração e validação do MORSYS2D. Este sistema 2D de modelação morfodinâmica simula os processos de transporte de sedimentos não-coesivos e a evolução batimétrica resultante em zonas costeiras. O sistema inclui um modelo de ondas (SWAN), um modelo de circulação (ELCIRC) e um modelo de transporte de sedimentos e de actualização de fundo (SAND2D). A aplicação, calibração e validação do MORSYS2D foi um procedimento sequencial, devido às inúmeras variáveis e processos envolvidos (como por exemplo, parâmetros de forçamento, fórmulas de transporte). Este procedimento iniciou-se com simulações forçadas apenas pela maré, e progressivamente foram adicionados os processos de agitação marítima e de transporte de sedimentos. Diferentes conjuntos de dados (níveis de água, velocidades, dados de ondas e batimetrias) foram utilizados para validar cada etapa. Simulações morfodinâmicas para campanhas de campo consecutivas, constituíram a validação final. De forma a investigar o efeito dos vários processos intervenientes na evolução morfodinâmica da embocadura (como por exemplo, agitação marítima e os caudais de cheia), foram realizadas simulações sintéticas. A partir da exploração do modelo, os resultados mostram que a variabilidade morfodinâmica da praia é condicionada principalmente pelas ondas, enquanto que o fluxo do rio domina a morfodinâmica da embocadura quando os fluxos de pico ocorrem. O sistema de modelos reproduz correctamente a hidrodinâmica (agitação marítima, níveis e velocidades), e produz previsões batimétricas qualitativamente correctas. Este estudo contribuiu para uma nova compreensão do sistema e da sua variabilidade.

keywords

Morphodynamic modeling, tidal inlets, Aljezur stream.

abstract

The morphology of tidal inlets is very dynamic, due to the combined action of waves, tides and river flows. The morphological changes of small and shallow inlets are particularly relevant, as even slight variations in the bathymetry may induce a dramatic effect on tidal propagation and distortion. Occasionally, these complex dynamics may lead to the closure of the inlet and thus degrade the water quality upstream. Numerical morphodynamic models constitute attractive tools to study these morphological changes, although their application is still time-consuming and requires a deep insight into the relevant processes. This study aims at analyzing the morphodynamics of the tidal inlet of a small and shallow coastal system (the Aljezur coastal stream), through the implementation, validation and exploitation of the MORSYS2D morphodynamic modeling system. The Aljezur stream is located in the south-west coast of Portugal and subject to the north Atlantic waves and winds, and tides along the Iberian shelf. The stream is about 36 km long, 1-3 m deep and 10-40 m wide. Five field campaigns were carried out between 2008-2010 to provide bathymetry, water levels, waves and currents, both in the estuary and the adjoining beach, for the understanding of the dynamics of the stream and for the application, calibration and validation of MORSYS2D. This 2D morphodynamic modeling system simulates the non-cohesive sediment transport processes and the resulting bathymetric evolution in coastal regions. The system includes a wave model (SWAN), a circulation model (ELCIRC) and a sediment transport and bottom update model (SAND2D). The application, calibration and validation of MORSYS2D were a step-by-step procedure due to the numerous variable inputs and processes involved (e.g., forcings, parameters, formulations). The procedure started with simulations forced only by the tide, and progressively were added the wave and sediment transport processes. Different data sets (water levels, velocities, wave parameters and bathymetries) were used to validate each step. Morphodynamic simulations conducted between consecutive field campaigns provided the final validation. In order to investigate the effect of the several processes on the morphodynamic evolution of the inlet (e.g., waves and peak river flows), synthetic simulations were performed. From the exploitation of the model, results show that the morphodynamic variability of the beach is dominated mostly by the waves while river flow dominates the morphodynamics of the inlet region when peak flows occur. The model system reproduces correctly the hydrodynamics (waves, levels and velocities), and produces predictions of bathymetry qualitatively correct. This study brought a new understanding of the system and its variability.

INDEX

| | | |
|-----|---|----|
| 1. | INTRODUCTION | 1 |
| 1.1 | MOTIVATION..... | 1 |
| 1.2 | OBJECTIVES..... | 4 |
| 1.3 | ORGANIZATION OF THE THESIS | 4 |
| 2. | STUDY AREA | 6 |
| 3. | SUPPORTING DATA ACQUISITION AND ANALYSIS | 10 |
| 3.1 | SUPPORTING FIELD CAMPAIGNS..... | 10 |
| 3.2 | DATA FROM THE SINES SEA STATION | 18 |
| 4. | THE MORPHODYNAMIC MODELLING SYSTEM MORSYS2D | 21 |
| 4.1 | GENERAL DESCRIPTION | 21 |
| 4.2 | THE CIRCULATION MODEL: ELCIRC..... | 22 |
| 4.3 | THE WAVE MODEL: SWAN | 23 |
| 4.4 | THE SEDIMENT TRANSPORT AND BOTTOM UPDATE/EVOLUTION MODEL: SAND2D..... | 23 |
| 5. | APPLICATION, CALIBRATION AND VALIDATION OF THE MODEL MORSYS2D | 24 |
| 5.1 | GENERAL PROCEDURE | 24 |
| 5.2 | TIDAL CIRCULATION | 25 |
| 5.3 | WAVE-INDUCED CIRCULATION | 31 |
| 5.4 | LOW FREQUENCY WATER LEVELS..... | 34 |
| 5.5 | MORPHODYNAMICS..... | 37 |
| 6. | EXPLOITATION OF THE MODEL | 42 |
| 6.1 | WAVES | 42 |
| 6.2 | HIGH RIVER FLOWS | 46 |
| 7. | DISCUSSION AND CONCLUSIONS | 52 |
| 8. | REFERENCES | 55 |

LIST OF FIGURES

| | |
|--|----|
| Figure 1 – Study site: a) location; b) bathymetry (in meters, relative to mean sea level); c) aerial photograph of the Amoreira beach and lower estuary (source: Google Earth); d) Amoreira beach; e) upstream end of the lower estuary. | 6 |
| Figure 2 – Division of the Aljezur stream by regions according to the type of sediments: A – lower estuary; B and C – mid-estuary; D – upper estuary; E – aquaculture ponds and salt marsh region; F – water treatment station (WTS) and Aljezur village. | 8 |
| Figure 3 – Location of the stations along the stream during campaign of May 2009. The bathymetry is colour-coded in meters, relative to mean sea level. | 11 |
| Figure 4 – Hydrodynamic data collected during the campaign in May 2009: a) free surface water level (relative to mean sea level) and b) velocities (positive values indicate flood). | 12 |
| Figure 5 – Wave data collected during the campaign in May 2009: a) station 11B; b) station 12; c) station 16; d) station 17 (relative to mean sea level). | 13 |
| Figure 6 – Bathymetry collected in the inlet and lower estuary a) May; b) June; c) July; d) September. The bathymetry is colour-coded in meters, relative to mean sea level. | 14 |
| Figure 7 – Amoreira beach photos taken between April 2008 and May 2009. | 15 |
| Figure 8 – Amoreira beach photos taken between April 2009 and March 2010. | 16 |
| Figure 9 – Amoreira beach photos taken between May and October 2010. | 17 |
| Figure 10 – The sediment samples collection: a) location and values of the D_{50} of the sediment samples at b) beach and c) stream inlet. | 18 |
| Figure 11 – Data from Sines from May to September 2009: a) sea surface elevation (relative to mean sea level); b) significant wave height; c) peak wave period; d) wave direction; e) wind intensity and direction and f) atmospheric pressure, recorded by the Portuguese Hydrographic Institute (IH) near the Port of Sines. | 19 |
| Figure 12 – Data used to calculate the values of water level fluctuations from May 2009: a) sea surface elevation (relative to mean sea level); b) atmospheric pressure; c) difference between predicted and the observed water level; d) water level fluctuation and e) correlation between the mean values of c) and e). | 20 |
| Figure 13 – Scheme for MORSYS2D. Only the models used in the present application are shown. | 22 |
| Figure 14 – Computational grid for ELCIRC and SAND2D: a) grid and bathymetry; b) detail of the beach and inlet area, c) lower estuary and d) salt marsh region near the aquaculture ponds. The bathymetry is colour-coded in meters, relative to mean sea level. | 26 |
| Figure 15 – Water level, comparison between data collected and the ELCIRC simulation results (relative to mean sea level). | 29 |
| Figure 16 – Velocity, comparison between data collected and the ELCIRC simulation results. | 30 |
| Figure 17 – Limits of the computational grids for SWAN and location of the WW3 outputs. | 31 |
| Figure 18 – Wave data from Sines and the boundary conditions from SWAN for May 2009. | 32 |

| | |
|---|----|
| Figure 19 – Wave parameters, comparison between data collected and the SWAN simulation results for station 11B and 12. _____ | 33 |
| Figure 20 – Comparison between the elevation model results with and without the effect of waves. _____ | 33 |
| Figure 21 – Boundary condition for the simulation for the period May 1 – 15 2009, without (A) and with (B) the effect of the water level fluctuations (WLF).: _____ | 35 |
| Figure 22 – Comparison between the water level data and the model results without (A) and with (B) the effect of the small water level fluctuations induced by the atmospheric pressure, for the period 9 th – 13 th May 2009, for the stations: a) 8 and b) 12. _____ | 35 |
| Figure 23 – Comparison between the water level data and the model results without (A) and with (B) the effect of the small water level fluctuations. _____ | 36 |
| Figure 24 – Comparison between the velocity data and the model results without (A) and with (B) the effect of the small water level fluctuations. _____ | 36 |
| Figure 25 – Initial conditions of bathymetry. The bathymetry is colour-coded in meters, relative to mean sea level. _____ | 38 |
| Figure 26 – Results from the sensitivity tests for the calibration of the sediment transport module. The bathymetry is colour-coded in meters, relative to mean sea level. _____ | 39 |
| Figure 27 – Bathymetry at the lower-estuary, inlet and beach on June 25 th 2009: a) data; b) model results. The bathymetry is colour-coded in meters, relative to mean sea level. _____ | 40 |
| Figure 28 – Bathymetry at the lower-estuary, inlet and beach on July 27 th 2009: a) data; b) model results. The bathymetry is colour-coded in meters, relative to mean sea level. _____ | 40 |
| Figure 29 – Difference between: a) final data and initial conditions and b) simulations results and initial conditions on June 25 th 2009. Positive (negative) values indicate erosion (accretion). ____ | 41 |
| Figure 30 – Difference between: a) final data and initial conditions and b) simulations results and initial conditions on July 27 th 2009. Positive (negative) values indicate erosion (accretion). ____ | 41 |
| Figure 31 – Initial bathymetry (12 th May 2009) and boundary conditions for the exploitation simulations: a) one tidal constituent and two tidal constituents for b) a spring tide and c) a neap tide. _____ | 42 |
| Figure 32 – Effect of the significant wave height (1, 2 and 3 m) and the wave direction (NW, W and SW) on the morphology of the Amoreira beach. See Table 5 for details. _____ | 44 |
| Figure 33 – Effect of the wave period (5, 10 and 15 s) and the wave direction (NW, W and SW) on the morphology of the Amoreira beach (see Table 5 for details). _____ | 45 |
| Figure 34 – Wave exploration results for a constant significant wave height ($H_s = 2$ m), constant wave period ($T = 10$ s) and with a variation of the wave direction (NW, W and SW), for a synthetic tide M2+S2. _____ | 46 |
| Figure 35 – Simulation results for the 7 th day of simulation of: a) constant river flow of $0.3 \text{ m}^3/\text{s}$ and to maximum peak flow of b) $1 \text{ m}^3/\text{s}$, c) $5 \text{ m}^3/\text{s}$, d) $10 \text{ m}^3/\text{s}$ and e) $15 \text{ m}^3/\text{s}$ during 10 h; and f) correspond to the location of the cross section analysis. The results correspond to the simulations with a synthetic tide M2. _____ | 47 |

Figure 36 – Results to the peak flow of 5 m³/s, during 5 (a, b and c), 10 (d, e and f) and 15 h (g, h and i). The results correspond to the 7, 10 and 15 days of simulation for a synthetic tide M2. _____ 48

Figure 37 – Results to the peak flow of 5 m³/s, during 10 hours. The results correspond to the 9, 11 and 15 days of simulation for a synthetic tide M2+S2. Neap tide (a, b, c) and spring tide: (d, e, f). _____ 49

Figure 38 – Analyze of the cross section at the inlet: a) evolution along the 15 days simulation for the different maximum peaks and a duration of 10 h, b) detail for the evolution with a constant river flow and a maximum peak of 1 m³/s and c) correlation between maximum flow volume and cross section for the different durations. _____ 50

Figure 39 – Cross sections results to each M2S2 versus river flow: a) a constant river flow of 0.3 m³/s during all simulation, and a peak flow of 5 m³/s during 10 hours, at the 9th day of simulation during a b) neap and c) spring tide _____ 50

LIST OF TABLES

| | |
|--|----|
| Table 1 – Main characteristics of the field campaigns. | 10 |
| Table 2 – RMS and Skill of the simulation results of water level and velocity for each station. | 30 |
| Table 3 – RMS and Skill of the simulation results of water level and velocity for each station. | 34 |
| Table 4 – Mean square error of the hydrodynamic simulation results of water level and velocities for each station. | 37 |
| Table 5 – Characteristics of the synthetic numerical tests for the wave forcing simulations. | 43 |

1. INTRODUCTION

1.1 MOTIVATION

Estuaries are among the most productive natural habitats in the world, along with the tropical rainforest and the coral reefs. Due to their unique characteristics, estuaries are a vital part of regional and global ecosystems. Many species of fish, birds, reptiles and mammals congregate to feed, find shelter, grow to adulthood, and stage migrations in estuaries, making these dynamic ecosystems rich in biodiversity of fauna and flora. Along with the ecological value, estuaries are also important economical regions for the local populations, providing natural resources through commercial and recreation activities.

Estuaries are semi-enclosed bodies of water formed in the transition zone between land and sea, where fresh water from rivers and coastal streams flows into and mixes with salt water of the ocean (Pritchard, 1967). These coastal systems are subject to both marine influences, through tides, waves and the influx of saline water; and riverine influences, through flows of fresh water and sediment.

The dynamics of estuaries depends on their size. Small estuaries exhibit some noteworthy differences relative to their larger counterparts. Because they are generally shallow, small absolute changes in bathymetry can represent large relative changes in the total depth. As a result, morphological variations may have a dramatic effect on tidal propagation and distortion, on hydrodynamics and, ultimately, on the transport and fate of water-borne material. For instance, some forcing conditions may induce severe reductions in the inlet cross-section, or even its closure, constraining the water renewal and putting public health at risk. Hence, the water quality in these systems depends strongly on their time-dependent morphologies (e.g., Oliveira *et al.*, 2007, 2010c).

This dependency justifies the need to assess the morphological behaviour of small estuaries and inlets in order to understand and study their water quality. However, the morphological behaviour is particularly difficult to simulate in small systems. First, some simplifications usually valid in large estuaries are inadequate in smaller ones. For instance, water level fluctuations due to wave setup or atmospheric pressure variations are typically neglected in circulation models of large estuaries. However, when the total

depth of an inlet is very small at low tide (e.g., below 1 m), these fluctuations may affect tidal propagation significantly. Secondly, space and time scales are highly correlated. A small estuary will also tend to evolve more rapidly than a larger one. While this faster evolution reduces the duration of the time series required to understand the variability of the system, it also increases the required sampling frequency, and often poses severe challenges to numerical morphodynamic models. Indeed, morphodynamic models are more prone to spurious oscillations when sediment fluxes are high (Fortunato and Oliveira, 2007).

Due to this complexity, the prediction and understanding of these morphological variations require sophisticated models, able to represent all the relevant processes involved, and with a detailed spatial representation. Numerical morphodynamic models constitute the most obvious choice, as they encapsulate the current knowledge of the hydrodynamic and sediment transport processes. They offer the possibility to assess different scenarios, test engineering solutions and investigate the importance of different processes.

However, in spite of recent advances, the development of these morphodynamic models is still in its infancy and their predictive capabilities remain limited (Bertin *et al.*, 2010). The poor scientific understanding of many processes and their interactions leads to many simplifications and parameterizations (e.g., many sediment transport formulae are available). Models include many possible options, and it is not always clear which ones are the most adequate for each application. Hence, existing models are difficult to apply due to the large number of choices available to the modeller. The modeller is required to have a thorough understanding of both the physical processes involved and the numerical methods used. In addition, successful applications of these models to tidal inlets are still scarce (Cayocca, 2001, Work *et al.*, 2001, Bertin *et al.*, 2009a, c, Plecha *et al.*, 2010). As a result, each new application raises new questions, and there is little guidance on the best procedure to apply, calibrate and validate these models.

The characteristics of the Aljezur coastal stream, located in the SW Portuguese coast, make it an ideal system to perform this kind of morphodynamic modeling. It is a small and shallow system with a very dynamic inlet subject to the combined action of

waves, tides and riverflows. Due to the small dimensions of the Aljezur stream, collecting the necessary data for the calibration and validation of the models is relatively inexpensive. Also this system is located in an important environmental protected area (Parque Natural do Sudoeste Alentejano e Costa Vicentina), where different and potentially conflicting uses exist, and the preservation of the water quality is a present concern.

Several authors have studied the Aljezur stream from a biological and geomorphological perspective (Magalhães *et al.*, 1987, Fidalgo e Costa *et al.*, 2002, 2003). Gama-Pereira (2005) performed a detailed geological study of the coastal system, characterizing the geomorphology of the stream and some physical aspects of the system. In particular, water level measurements along the stream showed that flood dominance increases from the coast upstream. The characterization of the drainage basin, soil occupation and use can be found in studies of land-use planning, performed to evaluate the effect of floods in the Aljezur village, due to extreme precipitations events (Almeida *et al.*, 2000). However, the morphodynamics of the Aljezur tidal inlet and of the Amoreira beach have not been studied. Hence, little is known about the processes controlling the morphology of the inlet.

In the scope of the project MADyCOS, other models have been applied to the Aljezur coastal system. Aiming at understanding the impact of the inlet variability on the distribution of contaminants, Oliveira *et al.* (2010c) performed particle simulations for two inlet configurations. In particular, these authors showed that the setup due to waves can promote sediment transport towards the head of the estuary. Also, a water quality model, ECOSELFE (Rodrigues *et al.*, 2009), was applied to study circulation (including salinity and temperature), the fecal contamination and the oxygen cycle in the stream (Rodrigues *et al.*, 2009, 2010), but did not account for the morphological evolution of the inlet. These authors highlighted the strong sensitivity of residence times to the wind and river flow. However, it remains unclear whether this sensitivity occurs in the whole estuary or only in the upper estuary, where tidal currents are weak.

In order to complement these studies, a morphodynamic understanding of the system is required, to identify the controlling physical processes that shape the inlet

configuration and ultimately help to evaluate the effect of the variability in the inlet in the water quality upstream.

1.2 OBJECTIVES

This work aims to contribute to the understanding of the physical (hydrodynamic and morphodynamic) processes that govern small coastal systems through the application, calibration and exploitation of the morphodynamic model MORSYS2D at the small Aljezur system. Simultaneously, it seeks to provide some guidance on how to approach the application and calibration of morphodynamic models to such systems.

This study was developed in the scope of the project MADyCOS (Multidisciplinary integrated Analysis of the sediment Dynamics and fecal contamination in intermittent Coastal Systems), which aims to provide a valuable and inexistent knowledge on the hydrodynamics, morphodynamics, residence times and sanitary condition in the Aljezur coastal stream, which is essential for its adequate management.

1.3 ORGANIZATION OF THE THESIS

In order to achieve the proposed objectives, three major tasks were undertaken:

Task 1 – Acquisition, processing and analysis of data of the Aljezur coastal stream:

- brief literature review of the main physical characteristics of the Aljezur stream, aiming to characterize the system for the implementation of the models;
- treatment and organization of the field data collected between 2008 and 2010, aiming at the implementation and validation of the models;

Task 2 – Implementation and calibration of the morphodynamic model for the Aljezur stream and adjacent coastal area:

- review of the numerical models to be used in the coastal system;
- application, calibration and validation of the wave model (SWAN);
- application, calibration and validation of the hydrodynamic model (ELCIRC);

- application, calibration and validation of the morphodynamic model (MORSYS2D) based on the calibration of the previous models and the sediment transport model (SAND2D);
- sensitivity analysis of the morphodynamic model.

Task 3 – Exploitation of the morphodynamic model:

- simulation of several scenarios that may occur in the study area;
- analysis of the relevant physical processes by establishing and testing hypotheses.

Based on the approach adopted, the thesis is organized in seven chapters:

Chapter 1: a general introduction of the work, describing the main objectives and the importance of this type of studies

Chapter 2: a brief characterization of the study area and the important factors which affect the morphological processes

Chapter 3: description and analysis of the relevant data collected during the field campaigns.

Chapter 4: brief description of the morphodynamic model and its various components

Chapter 5: application, calibration and validation of the models

Chapter 6: exploitation of the model

Chapter 7: discussion of the results and summary of main conclusions

2. STUDY AREA

The Aljezur stream (Figure 1) is a small coastal system subject to the action of winds, waves, tides and river flows, and is located in the southwest coast of Portugal (about 70 km south of Sines and 39 km north of Cape St. Vicente, Sagres).

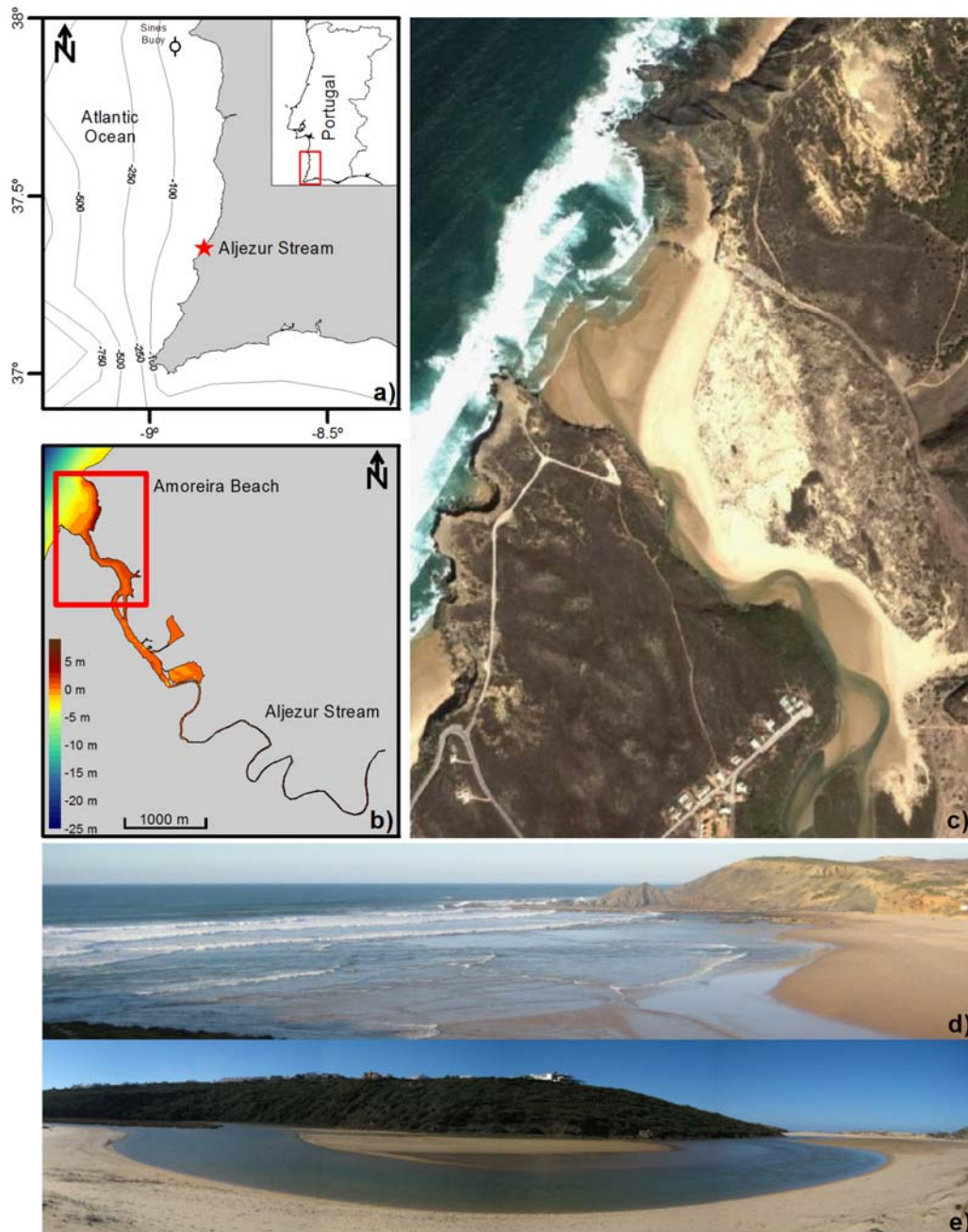


Figure 1 – Study site: a) location; b) bathymetry (in meters, relative to mean sea level); c) aerial photograph of the Amoreira beach and lower estuary (source: Google Earth); d) Amoreira beach; e) upstream end of the lower estuary.

The Portuguese coast is influenced by the North Atlantic winds and currents. The wind regime is an important factor in the climate of the region, with a strong maritime influence and with prevailing winds from the northern quadrant. The wave climate is severe, due to the exposure of the coast to the North Atlantic. Waves are predominantly from the NW/SW, with a mean significant wave height of 2 m. The ocean tides are semi-diurnal with maximum range of 4 m (Gama-Pereira, 2005).

The climate of the Aljezur region is mesothermal, with dry summers and occasional floods during the maritime winter (October to March). Despite the frequent floods during the months of highest rainfall, the streams usually present a low flow during most of the year, almost without natural drainage in drier seasons (Ribeiro *et al.*, 1994).

The whole stream is about 34 km long and drains a basin of about 182.9 km². It is formed by the Areeiro, Cercas and Alfambras streams, coming from the north, east and south, respectively. These streams connect near the village of Aljezur, running afterwards along the valley and connecting to the sea at the Amoreira Beach (Costa, 1993, in Gama-Pereira, 2005). The cross section of the stream varies along the valley. The stream is about 10-40 m wide and 1-3 m deep close to the inlet, and becomes narrower and slightly deeper in some regions upstream.

The Amoreira beach is about 600 m in the longshore direction and 300 m cross-shore. It is protected by rocky cliffs to the North and to the South and has a large field of coastal dunes. Aerial photographs from the last decades indicate that this dune field is propagating inland, progressively covering the salt marshes (Gama-Pereira, 2005).

The downstream part of the Aljezur stream is a small estuary, as it is influenced by both the tide and the freshwater flow. Although the inlet is usually connected to the sea, the closure of the inlet (which happened in April 1982 – November 1983; and in 1986) can occur in periods with exceptional wave, tide and flow conditions, isolating the stream from the sea and preventing the water renewal (Gama-Pereira, 2005).

Most of the year, the inlet is predominantly subject to the waves and tides, except in the short periods that follow extreme precipitations, which increase the flow and the river currents may overlap the effect of ocean conditions (Costa *et al.*, 1987, 1988). Therefore, the bathymetry configuration of the inlet is mostly determined by the balance

between tides and waves. During the wet months, strong riverflows can flush river sediments to the sea and contribute to the opening of the inlet (Gama-Pereira, 2005).

The tide is damped and distorted as it propagates upstream (Gama-Pereira, 2005). In terms of water levels, the system is flood-dominated, with ebbs significantly longer than floods (Gama-Pereira, 2005). However, because ebbs occur at lower tidal levels than floods, velocities are larger on ebb than on flood (Oliveira *et al.*, 2010c). Tidal asymmetry is also affected by the mean water level in the coast, for instance due to wave setup (Oliveira *et al.*, 2010c). Besides tides and river flow, the circulation in the estuary was shown to be affected by waves (Oliveira *et al.*, 2010c) and wind (Rodrigues *et al.*, 2010).

The distribution of the different size and type of sediments along the streams results from the different sediments transport agents (waves, tides, river flow and wind) and the sediments sources (river and sea) (Magalhães *et al.*, 1987). Gama-Pereira (2005) divided the Aljezur stream (from the inlet to the village of Aljezur) in four main regions, considering the type of sediments found in the superficial layer of the stream bed (Figure 2).

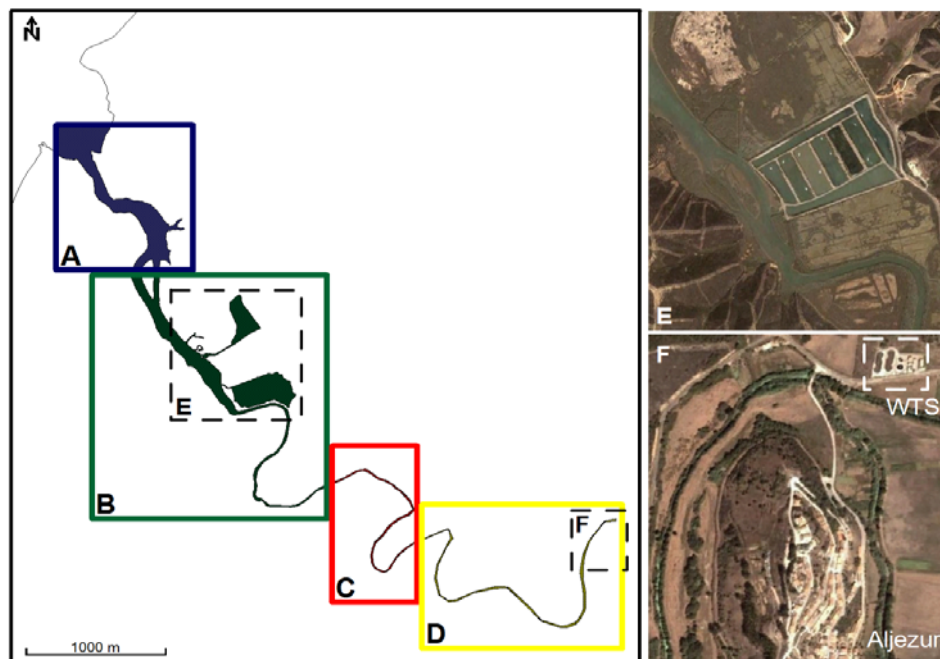


Figure 2 – Division of the Aljezur stream by regions according to the type of sediments: A – lower estuary; B and C – mid-estuary; D – upper estuary; E – aquaculture ponds and salt marsh region; F – water treatment station (WTS) and Aljezur village.

The first region (A) is composed exclusively of sandy sediments from marine origin; the second region (B) is mostly sludge, and includes extensive salt marshes; the third region (C) is a mix of sludge, gravel and sandy sediments and the last region (D) is mostly gravel with a small percentage of fine sediments. Based on this classification, we will adopt the following nomenclature: A – lower estuary; B and C – mid-estuary; D – upper estuary.

The anthropogenic action had an important role in shaping the Aljezur estuary, before it was integrated in the “Parque Natural do Sudoeste Alentejano e Costa Vicentina” in 1988. In the past, the valley was intensively occupied with rice fields, which covered most of the valley and constricted the margins of the stream. Nowadays, the former agriculture fields are mostly used for cattle pastures. The last human intervention happened in 1990 with the construction of aquaculture ponds in the salt marsh region (Figure 2 – E).

Currently, all the valley of the Aljezur stream and the Amoreira beach are established as a protected area, to safeguard the ecological interests of the zone. Due to its natural resources in fauna and flora, and attractive landscape, this region is being threatened by tourism, leading to a possible conflict between human and environmental interests. Therefore, all interventions in the catchment area are held only upstream of the water treatment station (Figure 2 – F). Downstream from this point, although still slightly constricted by the cattle pastures, the river currents can lead to small adjustments of the margins, especially during the rainy season.

3. SUPPORTING DATA ACQUISITION AND ANALYSIS

3.1 SUPPORTING FIELD CAMPAIGNS

This work is integrated in the project MADyCOS – Multidisciplinary integrated Analysis of the sediment Dynamics and fecal contamination in intermittent Coastal Systems. The general aim of this project is to improve the understanding of the effects of the morphodynamics of tidal inlets on the water quality of the associated estuaries.

The Aljezur coastal stream is an adequate system for this analysis due to its small dimensions, fast morphological dynamics and several contamination sources. Although the present work is mostly based on numerical modeling analysis, the implementation, calibration and validation of the models required extensive field data measured in different bathymetry settings and forcing conditions.

In order to characterize the hydrodynamics and the morphodynamics of the inlet of the Aljezur stream, four extensive field campaigns were conducted in 2008 and 2010 to measure bathymetry, water levels, waves and currents (Table 1). Between the two major campaigns in 2009, smaller campaigns were carried out to measure bathymetry alone. These campaigns aimed at collecting data to calibrate and validate the morphodynamic model. Other measurements were also carried out synoptically but their analysis is out of the scope of the present work. The reader is referred to Oliveira *et al.* (2010c) and Rodrigues *et al.* (2010) for these data and their analysis.

Table 1 – Main characteristics of the field campaigns.

| CAMPAIGN | | | TIDE | SEASON | BATHYMETRY | SEDIMENTS | STATIONS | | |
|----------|------|-----------|-------------|------------------------|------------|-----------|-------------|----------|------|
| | | | | | | | WATER LEVEL | VELOCITY | WAVE |
| ZERO | 2008 | MAY | Spring tide | End of maritime winter | ✓ | ✓ | 6 | 2 | 5 |
| ONE | | SEPTEMBER | Neap tide | End of maritime summer | ✓ | ✓ | 8 | 2 | 2 |
| TWO | 2009 | MAY | Mean tide | End of maritime winter | ✓ | ✓ | 9 | 2 | 4 |
| THREE | | SEPTEMBER | Spring tide | End of maritime summer | ✓ | × | 5 | 2 | 3 |

A preliminary analysis of the validity and completeness of the data sets revealed that the May 2009 campaign produced the best quality and most complete data sets. Therefore this chapter focuses on the description of the data collected during this field campaign and the bathymetries collected in the small campaigns between May and September of 2009. These data are later used in the application, validation and calibration of the models (Chapter 5). Further details about the field campaigns can be found in the technical reports of the field campaigns (Oliveira, 2009, 2010a, b; Freire, 2010b).

This chapter also summarizes the wave and meteorological conditions during May 2009, based on the data from the sea station “Buoys” in Sines.

Campaign Two was carried out between 11 and 13 of May, during mean tide in the end of maritime winter, for a whole tide cycle (13 hours). For this campaign, 11 stations were defined (Figure 3), distributed along the stream, from the Amoreira beach to the water treatment station. The stations were distributed in order to characterize the tide propagation, the incoming waves and the salinity intrusion.

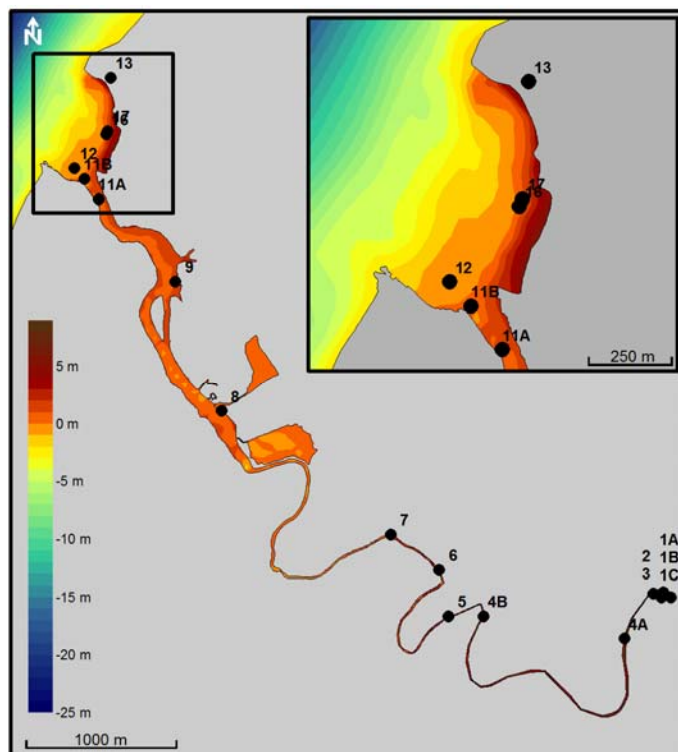


Figure 3 – Location of the stations along the stream during campaign of May 2009. The bathymetry is colour-coded in meters, relative to mean sea level.

Different instruments were used to collect the data. The water level fluctuations were measured at all stations through pressure sensors or rulers. Velocities at the inlet were measured using electromagnetic current meters (in stations 9 and 11A). The wave data were also measured with pressure sensors in the Amoreira beach (in stations 11B, 12, 14 and 17). Values were collected with different intervals of acquisition, depending on the nature of the target data. The data collected are summarized in Figures 4 and 5.

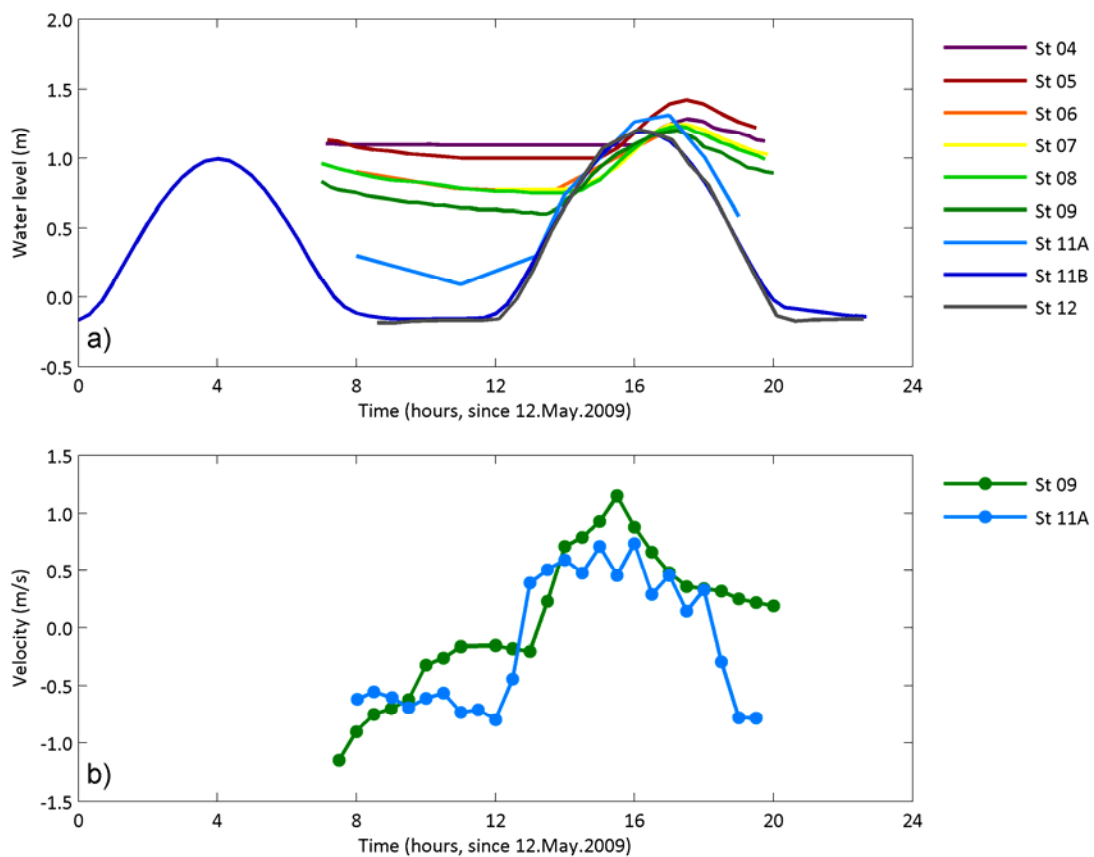


Figure 4 – Hydrodynamic data collected during the campaign in May 2009: a) free surface water level (relative to mean sea level) and b) velocities (positive values indicate flood).

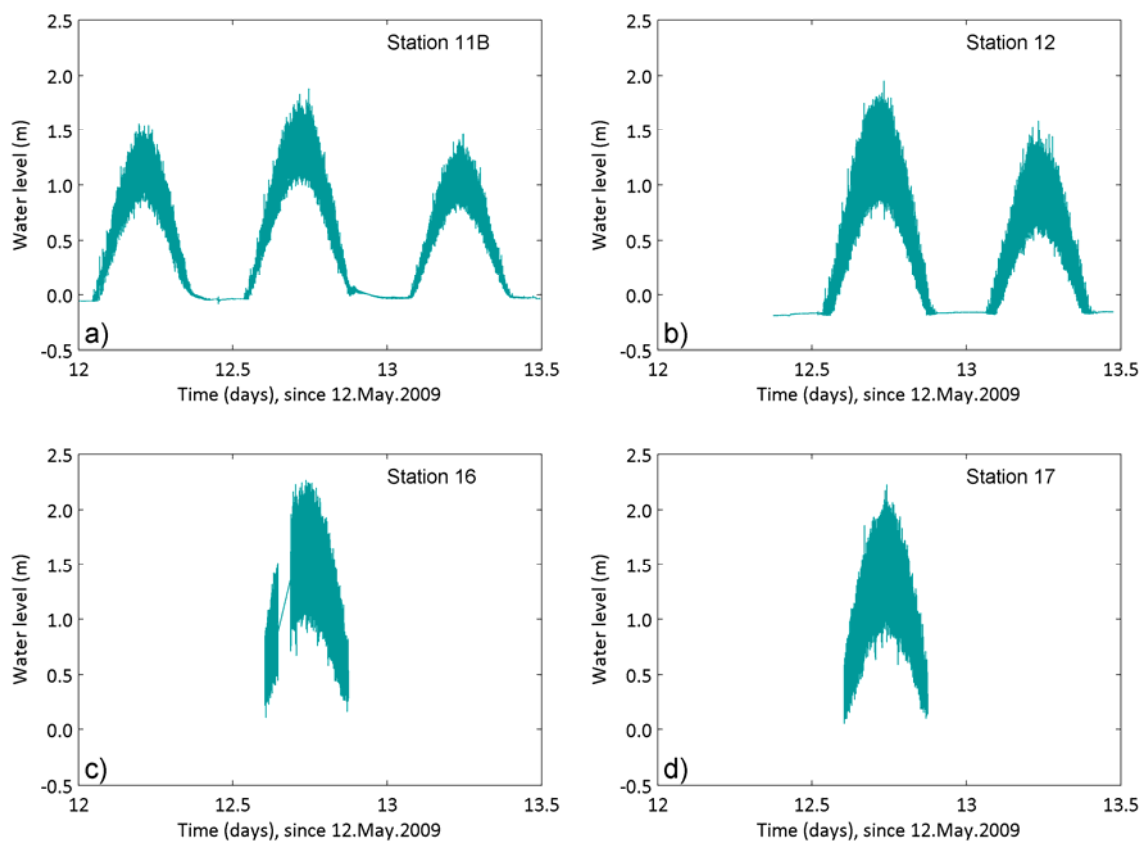


Figure 5 – Wave data collected during the campaign in May 2009: a) station 11B; b) station 12; c) station 16; d) station 17 (relative to mean sea level).

A complete bathymetric survey of the nearshore area and the Aljezur stream up to the limit of tidal propagation was performed during April 2008. In September 2008, another bathymetric survey of the nearshore area was performed in the scope of the project BAYBEACH (PTDC/CTE-GEX/66893/2006).

The Amoreira beach and the inlet bathymetry were measured during the four extensive field campaign. Between the two major campaigns in 2009, two smaller campaigns were made, targeting only bathymetry. The major surveys were performed in order to characterize the seasonal variability of the system and the smaller surveys to define the inlet geometry and its variation between late winter and late summer. The inlet topo-hydrographic data were measured using a total station and a DGPS. Figure 6 summarizes the data obtained. Due to some uncertainty, a few corrections in the bathymetry were performed, such as the removal of some points with unrealistic values and the improvement of the interpolation schemes.

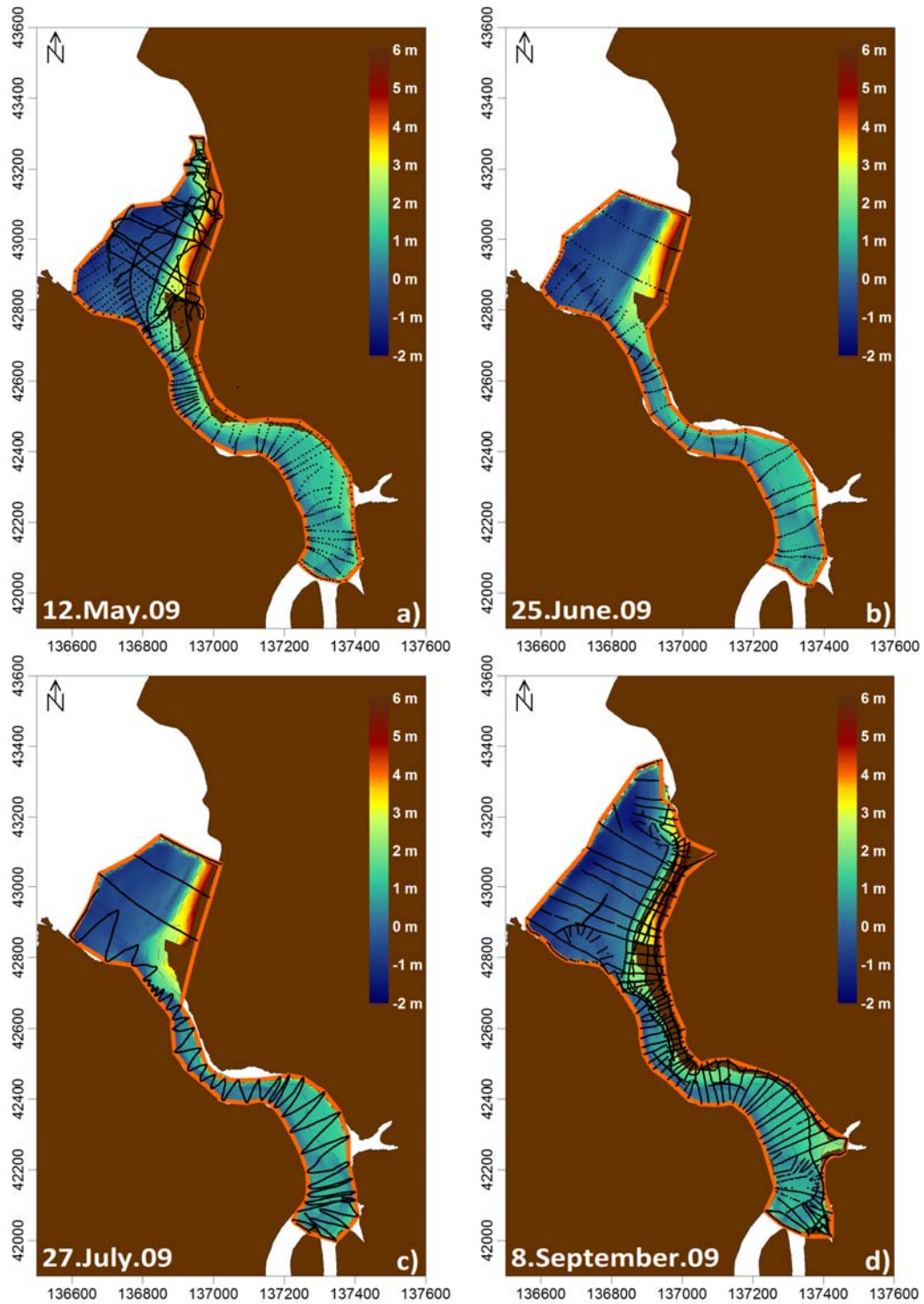


Figure 6 – Bathymetry collected in the inlet and lower estuary a) May; b) June; c) July; d) September. The bathymetry is colour-coded in meters, relative to mean sea level.

In addition to the bathymetry data, several photos were taken to the Amoreira beach from station 13 (Figure 3) and nearby locations, between April 2008 and September 2010 (Figure 7 to Figure 9).



Figure 7 – Amoreira beach photos taken between April 2008 and May 2009.



Figure 8 – Amoreira beach photos taken between April 2009 and March 2010.



Figure 9 – Amoreira beach photos taken between May and October 2010.

The bathymetric data in the lower estuary and the Amoreira beach photos indicate that there is a significant variability of the configuration of the main channel of the stream, especially in the inlet region. Although shallow depths were measured in the inlet during the data and photos acquisition, the stream was never isolated from the ocean.

Sediments samples were collected in the Amoreira beach and in the lower estuary, and analysed in laboratory to determine their grain size distribution (Figure 10). The samples were collected in the main morphosedimentary units (beach, dune field, sand bar, estuary, inlet, salt marsh). Results reveal a strong uniformity in the sediment size, with $D_{50} = 0.3$ mm (Freire *et al.*, 2010a).

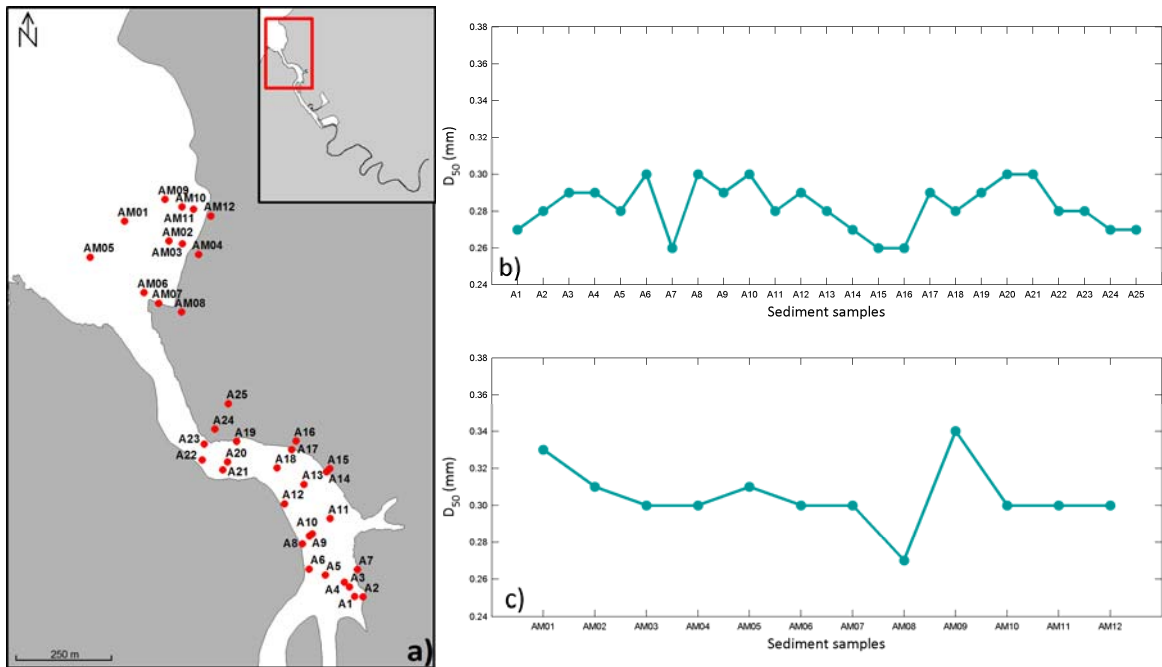


Figure 10 – The sediment samples collection: a) location and values of the D_{50} of the sediment samples at b) beach and c) stream inlet.

3.2 DATA FROM THE SINES SEA STATION

Data from the sea station in Sines were also analysed in order to determine the boundary conditions for the tidal model. In addition, these data provided a validation of the boundary conditions used to force the wave model. The Sines buoy is located at 97 m depth, at the coordinates $37^{\circ}55'16''N$ $8^{\circ}55'44''W$ (Figure 1). Figure 11 summarizes the sea and meteorological conditions registered from May to September of 2009 in Sines.

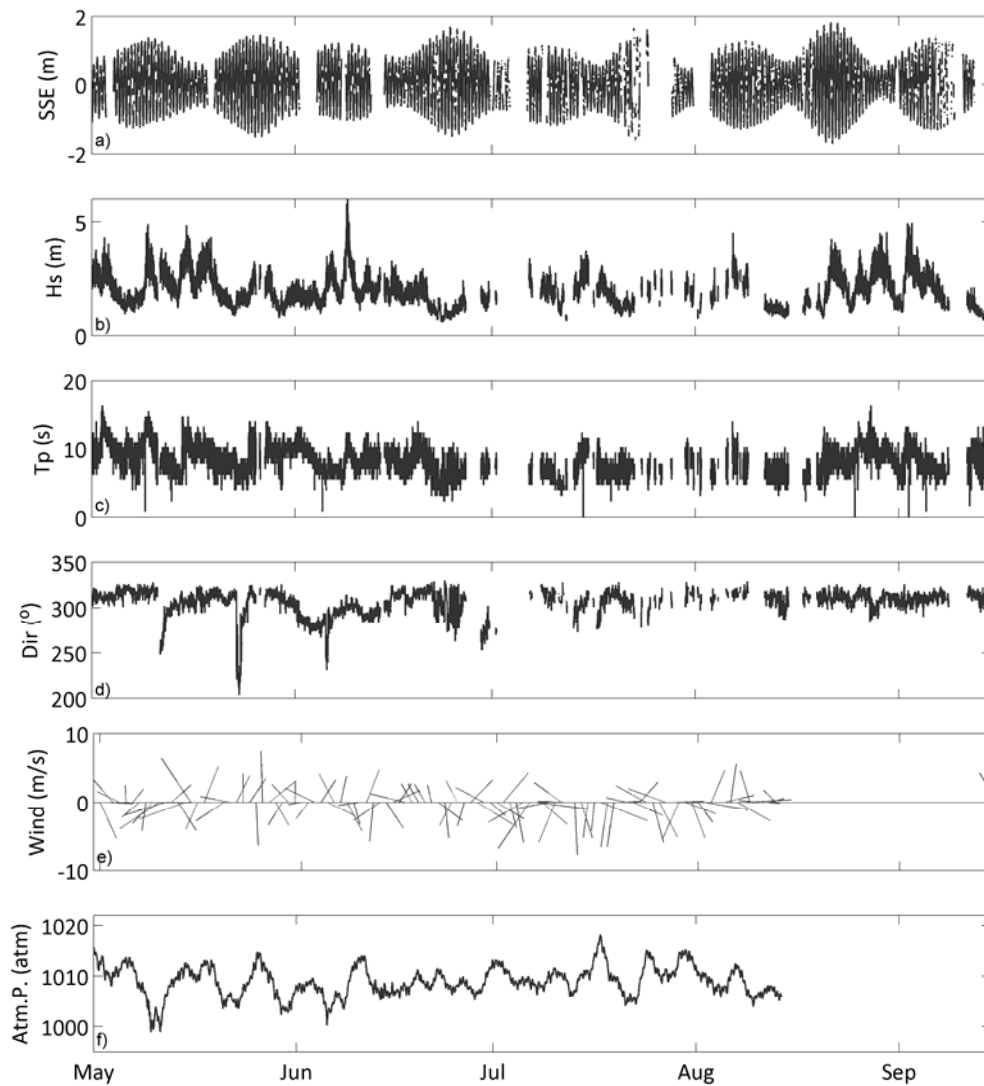


Figure 11 – Data from Sines from May to September 2009: a) sea surface elevation (relative to mean sea level); b) significant wave height; c) peak wave period; d) wave direction; e) wind intensity and direction and f) atmospheric pressure, recorded by the Portuguese Hydrographic Institute (IH) near the Port of Sines.

As already mentioned, small fluctuations in the water level associated with meteorological phenomena are usually neglected in deeper coastal systems. However, in shallower systems, these fluctuations can be significant relative to the total depth. Therefore, to evaluate the effect of these fluctuations, the values of atmospheric pressure (Figure 12b) were converted in to values of low frequency water level (Figure 12d) through the expression:

$$P(t) - \langle P \rangle = \rho \cdot g \cdot (Z0(t) - \langle Z0 \rangle),$$

where $P(t)$ is the observed atmospheric pressure, $\langle P \rangle$ is the mean atmospheric pressure, $Z_0(t)$ is the real water level, $\langle Z_0 \rangle$ is the mean sea level, ρ is the sea water density and g is gravity. Using the difference between the sea surface elevation predicted by harmonic synthesis and the observed one (Figure 12c) and the values of water levels fluctuations, the correlation between these two variables was calculated (Figures 12e).

Results (Figure 12e) show a very high correlation between the two signals ($R^2 = 0.905$). The correlation function was therefore used in the model calibration and validation to infer the water level fluctuations from atmospheric pressure data as a boundary condition.

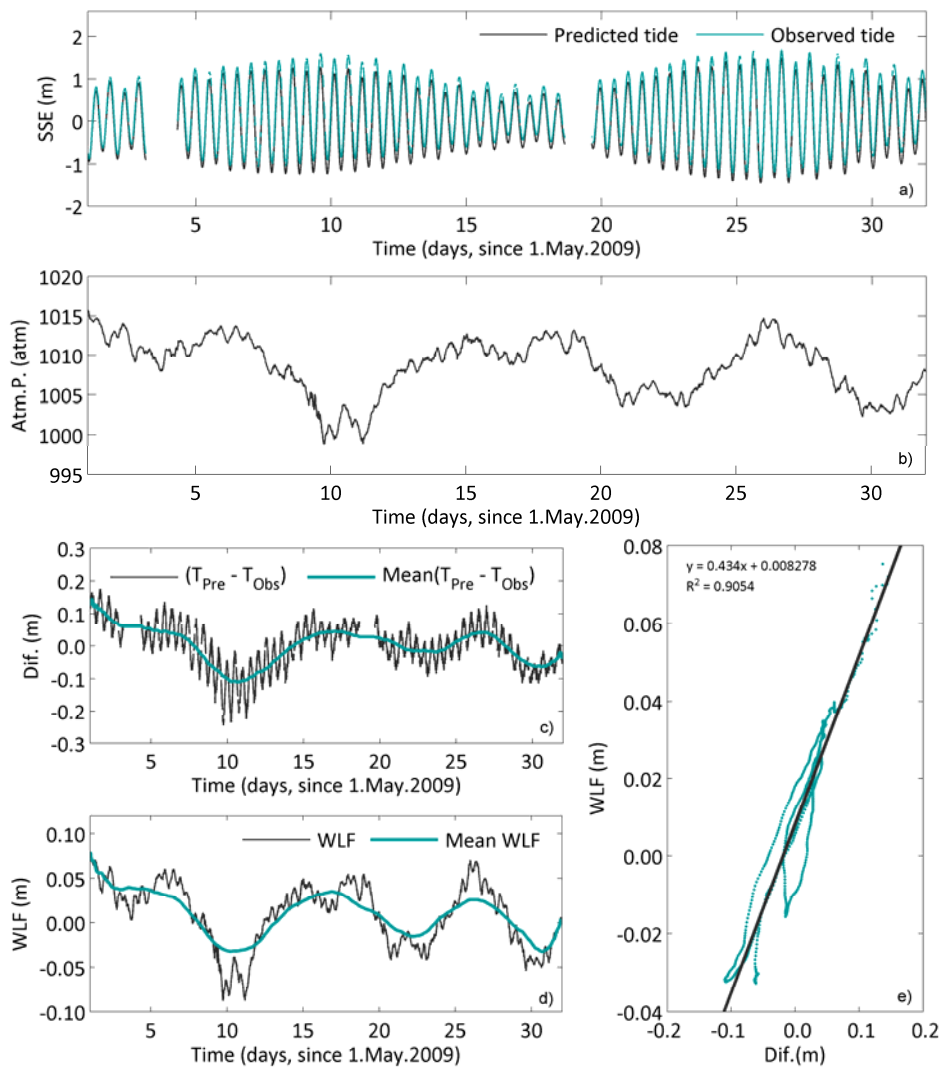


Figure 12 – Data used to calculate the values of water level fluctuations from May 2009: a) sea surface elevation (relative to mean sea level); b) atmospheric pressure; c) difference between predicted and the observed water level; d) water level fluctuation and e) correlation between the mean values of c) and e).

4. THE MORPHODYNAMIC MODELLING SYSTEM MORSYS2D

4.1 GENERAL DESCRIPTION

The 2D morphodynamic modelling system MORSYS2D simulates the non-cohesive sediment transport processes and the resulting bathymetric evolution, forced by tides, wind, river flows and waves (Fortunato and Oliveira, 2004, Bertin *et al.*, 2009b). MORSYS2D was developed for coastal regions, with a focus on tidal inlets.

The present version of MORSYS2D, driven by waves and tides, has been applied with success at three tidal inlets: Ancão (Bertin *et al.*, 2009a), Óbidos lagoon (Bertin *et al.*, 2009c; Bruneau *et al.*, 2010) and Santo André lagoon (Nahon *et al.*, 2010). Several other applications were carried out, either driven by tides alone (e.g., Fortunato and Oliveira, 2004; Plecha *et al.*, 2010), or to synthetic cases (Nahon *et al.*, 2009). The model has proven to be able to predict physical processes such as the formation of meanders, the migration of tidal inlets and the generation of sand bars (Bruneau *et al.*, 2010), and its predictions agree with the extensive empirical knowledge and models (Nahon *et al.*, 2009).

MORSYS2D consists of a C-shell script that runs independent models of waves, circulation, sediment transport and water quality, controlling the transfer of information between them and performing control checks (Figure 13). Computational efficiency is sought through the use of an adaptive time stepping procedure (Bertin *et al.*, 2009b), the partial use of parallel codes (Bruneau *et al.*, 2010), and the optimization of information transfer between modules (Costa *et al.*, 2010).

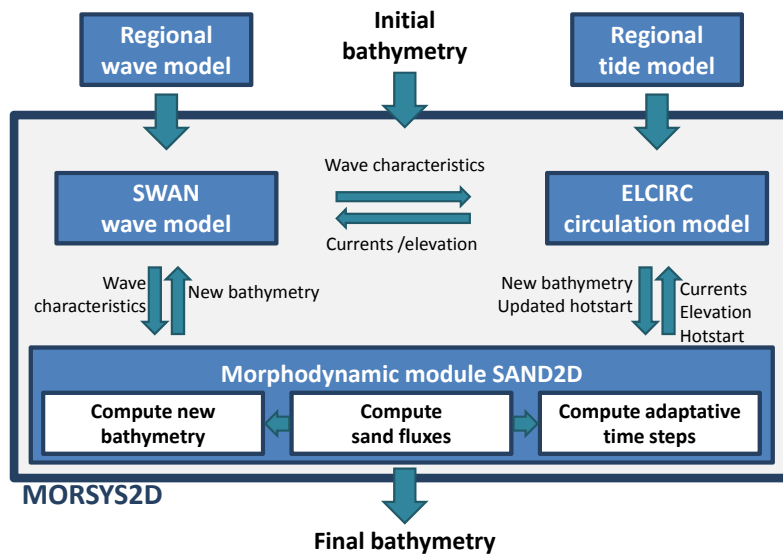


Figure 13 – Scheme for MORSYS2D. Only the models used in the present application are shown.

This modelling system has been developed at LNEC and offers a choice between different modules for waves and currents. At present, it has two hydrodynamic models (ADCIRC – Luetlich *et al.*, 1991, and ELCIRC – Zhang *et al.*, 2004), two wave models (REF/DIF1 – Kirby and Dalrymple, 1994, and SWAN – Booij *et al.*, 1999), and a sediment transport and bottom update model (SAND2D – Fortunato and Oliveira 2004; 2007c).

In this chapter, only the modules used in this study are briefly described. A detailed description of previous and present versions of the model are given in Fortunato and Oliveira (2004; 2007a), Bertin *et al.* (2009a) and Bruneau *et al.* (2010).

4.2 THE CIRCULATION MODEL: ELCIRC

ELCIRC (Zhang *et al.*, 2004) is a 3D baroclinic circulation model, which solves the shallow water equations through a combination of Eulerian–Lagrangian methods and finite volumes on unstructured grids. ELCIRC is an open source model developed at the Centre for Coastal Margin Observation and Prediction (www.stccmop.org/CORIE/modeling/elcirc/index.html). This model was developed for simulations from ocean to small river scales, considering the several physical processes due to the different atmospheric, ocean and river forcings.

Within MORSYS2D, ELCIRC is run with a single vertical layer, i.e., in 2D depth-averaged model (Bertin *et al.*, 2009a). The possibility of using unstructured grids allows local grid refinements, resulting in better results with low computational costs.

4.3 THE WAVE MODEL: SWAN

The 3rd generation numerical wave model SWAN (Booij *et al.*, 1999) solves the spectral action balance equation with sources and sinks. SWAN is used to simulate the wave propagation from deep to shallow water regions.

This spectral model accounts for the processes of generation, propagation and dissipation of waves, forced by wind, including refraction and diffraction, bottom friction and wave breaking (The SWAN team, 2010). In MORSYS2D, SWAN is used with structured grids and in stationary mode (Bertin *et al.*, 2009a).

4.4 THE SEDIMENT TRANSPORT AND BOTTOM UPDATE/EVOLUTION MODEL: SAND2D

SAND2D is the sediment transport and bottom update model used in MORSYS2D. It uses the information of waves and currents, provided by the hydrodynamic models, to compute the sand fluxes through one of the several empirical formulas implemented. Solving the Exner equation, the model computes the final bathymetry for each time step (Fortunato and Oliveira, 2004; 2007a). The time step can be specified by the user or adjusted automatically to approach a target Courant number of 1 (Bertin *et al.*, 2009a).

The Exner equation is solved on an unstructured grid. While MORSYS2D offers the possibility to use different grids for flow and transport, it is used here the same grid for ELCIRC and SAND2D to minimize interpolations and improve computational efficiency. The model also offers several filters to avoid the typical numerical problems of the morphodynamic models (Fortunato and Oliveira, 2007b).

5. APPLICATION, CALIBRATION AND VALIDATION OF THE MODEL MORSYS2D

5.1 GENERAL PROCEDURE

Because MORSYS2D combines several models, its application, calibration and validation is a lengthy procedure. In particular, the variable inputs are too numerous to vary simultaneously: forcings (e.g., river flow, waves), parameters (e.g., friction coefficient, wave breaking coefficient), geometry description (e.g., grids, bathymetry interpolators), formulations (e.g., sediment transport formulation), numerical formulations (e.g., bathymetric filters), etc. In addition, the number of manageable simulations is limited by the high CPU costs: typical morphodynamic simulations in the Aljezur stream run at 30% of real time, when run in serial mode.

To deal with these difficulties, a step-by-step procedure was adopted, starting with the simplest simulations, and progressively adding more processes and models. This approach allowed the calibration of one model at the time, using data from the stations to validate each new step and where neglecting some physical processes seemed acceptable (e.g., wind). Still, the number of parameters and other input choices prevented a full optimization of the model setup.

This chapter summarizes the process of application, calibration and validation of the MORSYS2D. The procedure was the following:

1. First the circulation model was implemented. The computational grid and the bathymetry interpolation were verified by forcing the model only with tides and river flow. Sensitivity analyses coupled with field campaigns led to adjustments in the model domain and friction coefficients. Preliminary values for the unknown mean sea level for each campaign were also determined in the calibration phase.
2. Coupled tide / wave simulations were conducted next. At this stage, the breaking formulation and parameter were selected through a comparison with wave data.

3. The circulation model was then further tuned by including atmospheric pressure effects at its ocean boundary. A final validation of the wave and tidal models was carried out.
4. Morphodynamic simulations, forced by waves and currents, were performed next. The sediment transport formula and the filtering parameters were selected to avoid spurious oscillations and other non-physical behaviours. And finally, morphodynamic simulations between consecutive field campaigns were conducted to assess the performance of the model.

These various steps are described in detail below.

5.2 TIDAL CIRCULATION

The bathymetry used in the simulations combines several sets of available data: data collected in the scope of the project BAYBEACH in September 2008 in the external zone in front of the Amoreira beach; data collected during the May 2009 field campaign for the beach, inlet and lower estuary area; data collected by the Hitop campaign in April 2008 for the mid- and upper-estuary; and data measured on September 2009 in the salt marshes.

Based on the available data, bathymetries and aerial photographs, an unstructured grid for ELCIRC and SAND2D was created using SMS, xmgredit (Turner and Baptista, 1993) and the grid post-processor of Fortunato *et al.* (2010) (Figure 14). The grid extends from the water treatment plant, where river flows were measured, to 9 km away from the inlet. The grid covers the Aljezur stream downstream of the water treatment station, most of the salt marshes region, the Amoreira beach and the offshore area up to a maximum depth of 65 m. To ensure the propagation of the tide upstream, several refinements were required in the inlet and estuary region, resulting in a grid with a spatial resolution ranging from 2.5 m to 500 m. These refinements also ensured a better resolution in the morphological changes in the area of interest. In spite of the small extent of the system, the final grid has approximately 40000 nodes due to the very high resolution required to represent the narrow inlet and the breaking zone. The weak

bathymetric filter of Fortunato and Oliveira (2000) was used to eliminate small-scale bathymetric features unresolved by the grid.

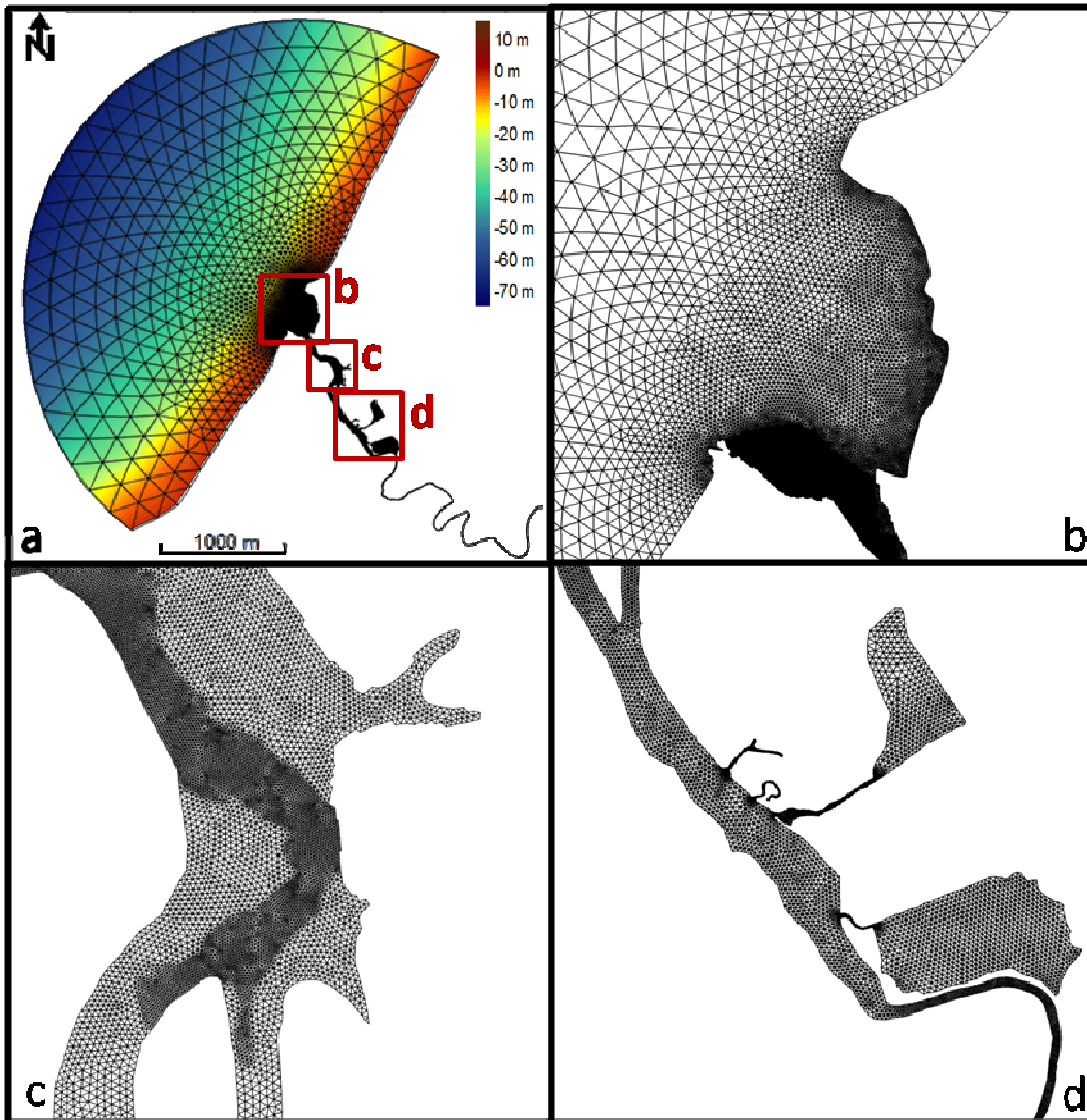


Figure 14 – Computational grid for ELCIRC and SAND2D: a) grid and bathymetry; b) detail of the beach and inlet area, c) lower estuary and d) salt marsh region near the aquaculture ponds. The bathymetry is colour-coded in meters, relative to mean sea level.

The first simulations were performed for 15 days (starting on 1st May 2009), with a constant time step of 5 s. The model was forced at the ocean boundary by eleven tidal constituents (Z0, O1, K1, M2, S2, N2, K2, M4, MN4, MS4 and M6), taken from a regional tidal model (Fortunato *et al.*, 2002), and by a constant flow of 0.3 m³/s at the river boundary. This value was based on the data measured during the May 2009 field campaign. The values of Z0 taken from the regional model are very small (of the order of

a few millimetres). However, they are retained as their gradients generate residual currents in the coastal zone.

Since computational time is a major concern, an artificial hotstart file is generated at the beginning of each simulation, allowing a faster equilibrium of the system which starts with a fully inundated domain, rather than a constant level, cold-start conditions.

The velocity and water levels simulations results were compared with field data at stations 4, 5, 6, 7, 8, 9, 11B and 12 (Figure 3).

Several sensitivity tests were performed to calibrate the model and verify the sensitivity to parameters variations. One of the first parameters to be tested was the variation of the mean sea level value. This is a key factor in the variation of the propagation of the tide along the stream, because a higher sea level promotes the propagation of the tide further upstream. To simulate these variations, different mean sea levels were considered at the oceanic boundary: 2.10, 2.15 and 2.20 m. These values were added to the Z0 amplitudes taken from the regional model. Based on the analysis of data from Sines (average of the period 2008 – 2009), the mean sea level is about 20 cm above the official value from 1970 (i.e., the mean sea level is now 2.20 m above chart datum). The comparison between data and the results of simulations for this period revealed that the optimum value for May 2009 is only 15 cm above this official value, showing the possible influence of other factors which occur during the period of the campaign along with the setup due to waves.

The second parameter to be tested was the drag coefficient (or Manning coefficient), varying values from 0.01 to 0.02 $\text{m}^{1/3}/\text{s}$ (with a step of 0.002 $\text{m}^{1/3}/\text{s}$), constant in the entire domain. These values were based on the sediment type present in the Aljezur stream (Figure 2). The lowest value led to better results (especially at the upstream stations), although the value of 0.01 $\text{m}^{1/3}/\text{s}$ is unrealistic for the lower estuary and beach regions where bottom sediments are exclusively sand and large bedforms occur. In order to solve this problem, other simulations used a drag coefficient variable in space, with 0.01 $\text{m}^{1/3}/\text{s}$ in the upper- and mid-estuary, where bottom sediments are mostly sludge, and 0.02 $\text{m}^{1/3}/\text{s}$ elsewhere. These last tests with the drag coefficient

showed that the values used in the inlet zone are the ones that mostly affect the propagation of the tidal wave upstream.

The third parameter to be tested was the effect of the variation of the stream flow. The values used range from 0.1 to 0.5 m³/s and are based on the data collected during field campaigns. This test demonstrated that the lower values of river flow allowed the tide to propagate further upstream.

During these sensitivity tests a setup of 0.10 m was used to simulate the effect of waves. The increase of this value revealed the importance of the setup of waves in the propagation of the tide inside the stream.

Figures 15 and 16 present the final simulation results with best comparison with the data collected in May 2009.

To evaluate the performance of the model, the root mean square error (RMS) and the predictive skill were calculated between the observed data and the simulation results:

$$RMS = \left\{ \frac{1}{N} \sum_{i=1}^N [\xi_d(t_i) - \xi_m(t_i)]^2 \right\}^{\frac{1}{2}}$$

where $\xi_d(t)$ and $\xi_m(t)$ are the observed data and model results, respectively and N is the number of measurements in the time series,

$$Skill = 1 - \frac{\sum |\xi_m - \xi_d|^2}{\sum (|\xi_m - \bar{\xi}_d| + |\xi_d - \bar{\xi}_d|)^2}$$

where $\bar{\xi}_d$ represents the time mean of the observed data.

RMS values scaled by the local tidal amplitude are considered excellent when they are lower than 5 % and very good when they are between 5 % and 10 % (Dias *et al.*, 2009). When considering the predicted skill, the values closer to 1 classified the model results in perfect agreement with the observed data, while values near 0 demonstrate the opposite.

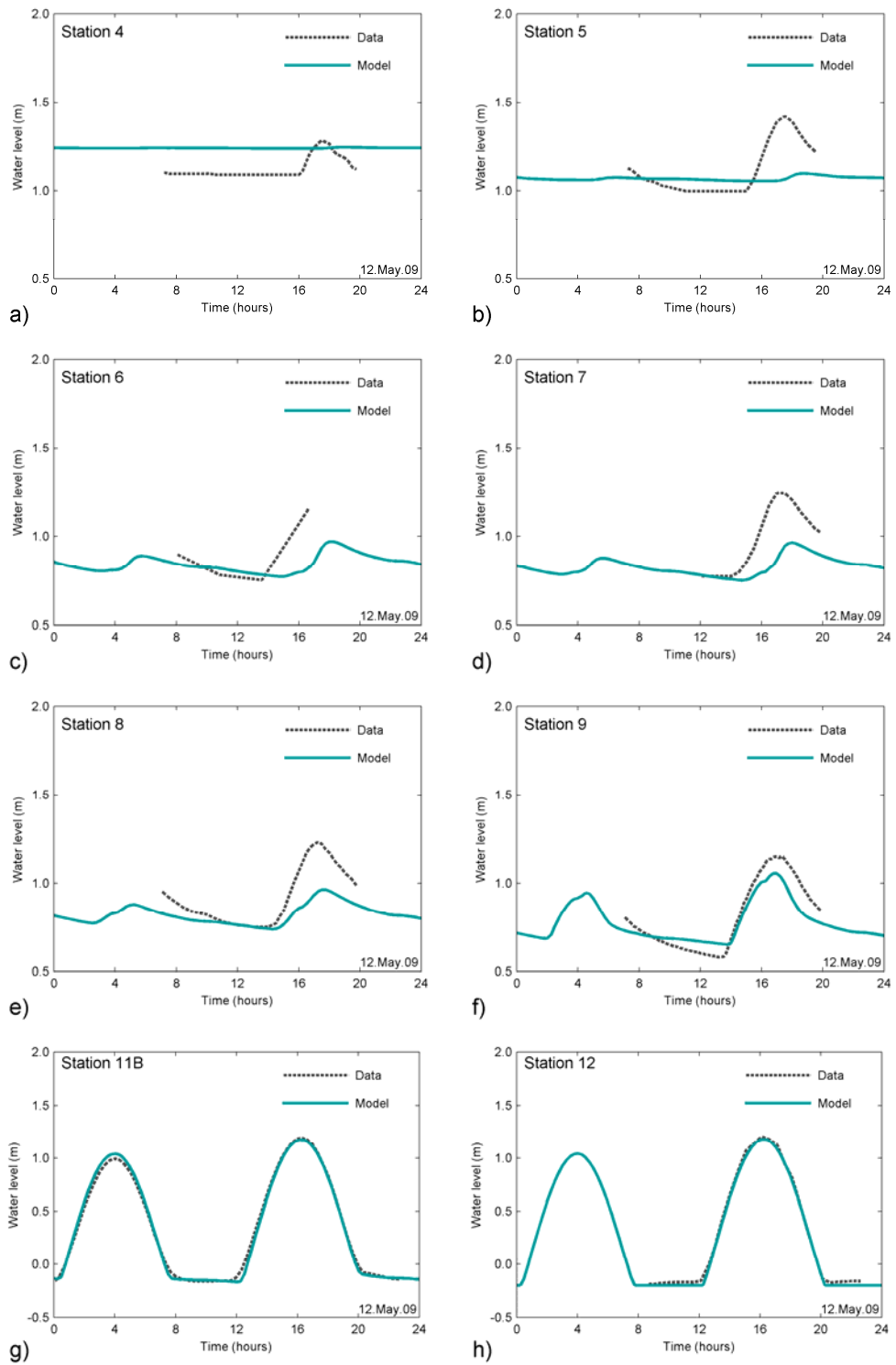


Figure 15 – Water level, comparison between data collected and the ELCIRC simulation results (relative to mean sea level).

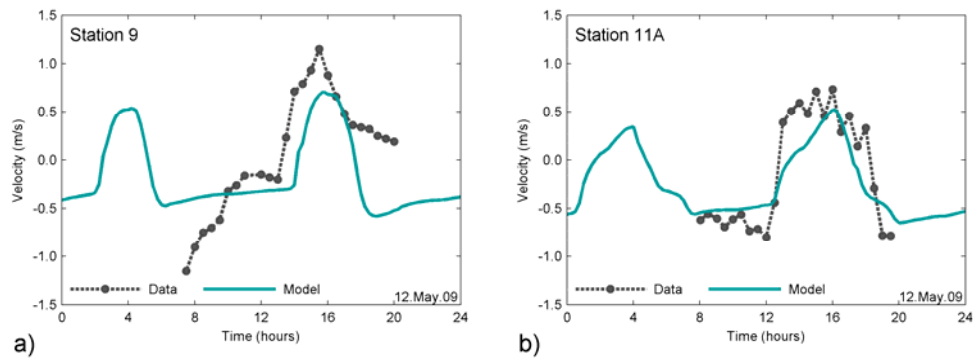


Figure 16 – Velocity, comparison between data collected and the ELCIRC simulation results.

From the results of these tests several parameters was determined to be used henceforth. The values that led to the best results were 2.15 m for the mean sea level and the drag coefficient variable in space (between values of 0.01 in the upper and mid estuary and 0.02 in the lower estuary). The sensitivity test to the river flow, showed the sensitivity of the model to this parameter. In spite of this fact, the value of 0.3 m/s measured in May 2009 was established to be used in futures simulations. Table 2 summarizes the RMS and performance Skill for each station, for the final simulation results with best similarity with the data.

Table 2 – RMS and Skill of the simulation results of water level and velocity for each station.

| | Station | RMS (m) | Skill |
|-------------|---------|---------|-------|
| Water Level | 4 | 0.140 | 0.037 |
| | 5 | 0.129 | 0.404 |
| | 7 | 0.131 | 0.824 |
| | 8 | 0.090 | 0.887 |
| | 9 | 0.058 | 0.972 |
| | 11B | 0.031 | 0.999 |
| | 12 | 0.025 | 0.999 |
| Velocity | 9 | 0.513 | 0.528 |
| | 11B | 0.303 | 0.825 |

Both the RMS and the skill show the excellent performance of the model at the stations closer to the ocean (station 11B and 12), and a decreasing accuracy towards the head of the stream, possibly due to the several limitations of the bathymetric data.

5.3 WAVE-INDUCED CIRCULATION

SWAN was run with two nested grids, to propagate waves from offshore to the inlet. The first grid is 17.5 km long and 14.8 km wide, and has a constant spacing of 200 m (about 7000 nodes). The second grid is curvilinear, with a maximum resolution in the surf zone and in the inlet, with spacings between 3 and 25 m. It is 1.7 km long and 1.2 km wide and covers an area of 21 km², with approximately 11000 nodes (Figure 17).

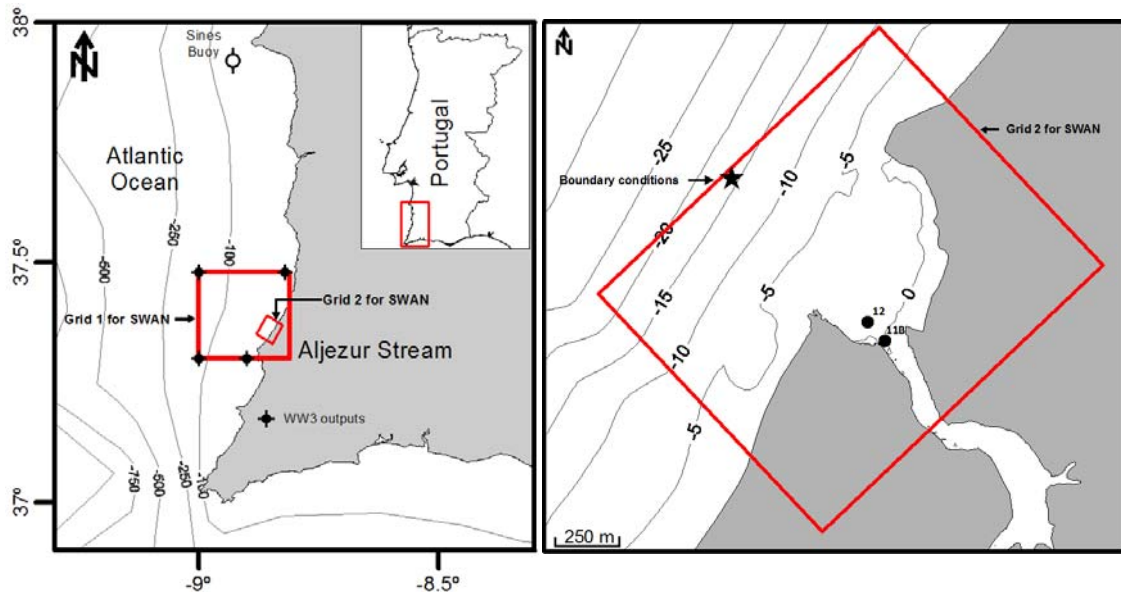


Figure 17 – Limits of the computational grids for SWAN and location of the WW3 outputs.

The boundary conditions for the coarser grid were provided by results from the regional wave model WW3 of Dodet *et al.* (2010). SWAN was run every 20 min, being forced at the final grid by the boundary conditions from the coarser grid and water levels from ELCIRC.

These simulations were performed for the period of 8-14 May 2009, using the coupled hydrodynamic component of MORSYS2D, so that the water level variations were provided by the previously calibrated ELCIRC and the radiation stresses from SWAN are used to force ELCIRC.

SWAN was calibrated for the parameters of breaking (0.5 – 0.8), dissipation rate (0.5 – 1.5) and variation of the beach slope (0.01 – 0.04), through comparisons with measured significant wave height (H_s), and mean wave period (T). Boundary conditions were validated against data from the Sines buoy (Figure 18)

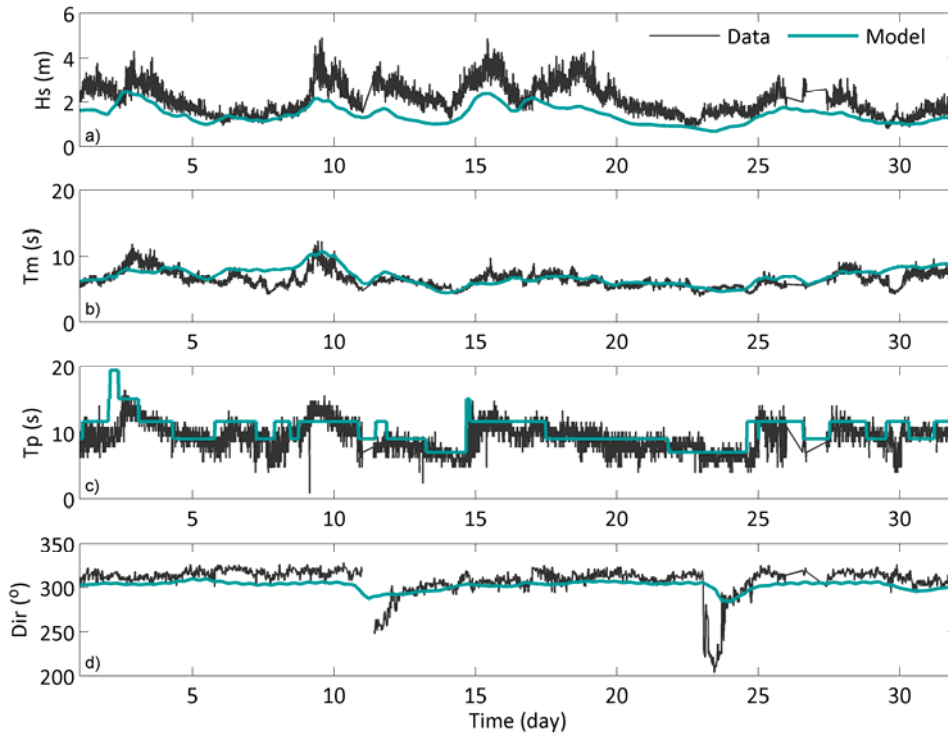


Figure 18 – Wave data from Sines and the boundary conditions from SWAN for May 2009.

The model results reveal a good agreement with the data from Sines. Some discrepancies between the model and the data may be due to the different location and depth of the buoy relative to the point where model results were taken (in front of Amoreira beach at 15 m depth).

From the sensitivity tests, the parameters which led to the best results were a constant breaking parameter of 0.8 and a dissipation rate of 0.5. These values are used henceforth in the calibration of sediment transport model.

Figure 19 presents the final simulation results with the best similarity with the wave data for the stations 11B and 12. Figure 20 shows the water level results for the simulations with and without waves, for stations 5, 8, 9 and 12.

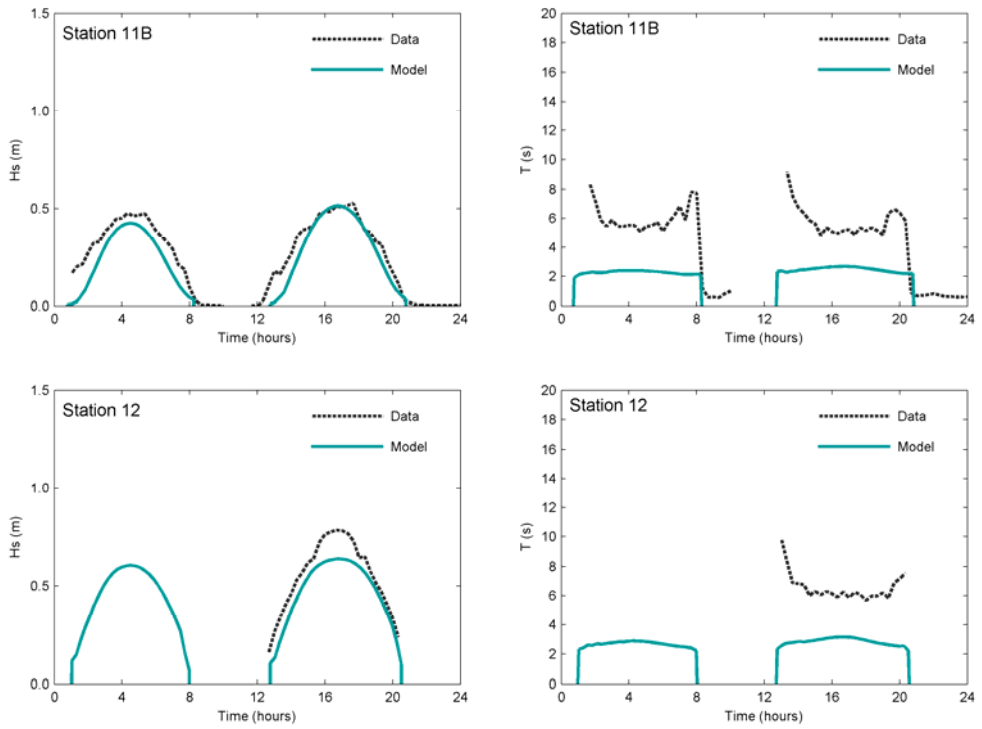


Figure 19 – Wave parameters, comparison between data collected and the SWAN simulation results for station 11B and 12.

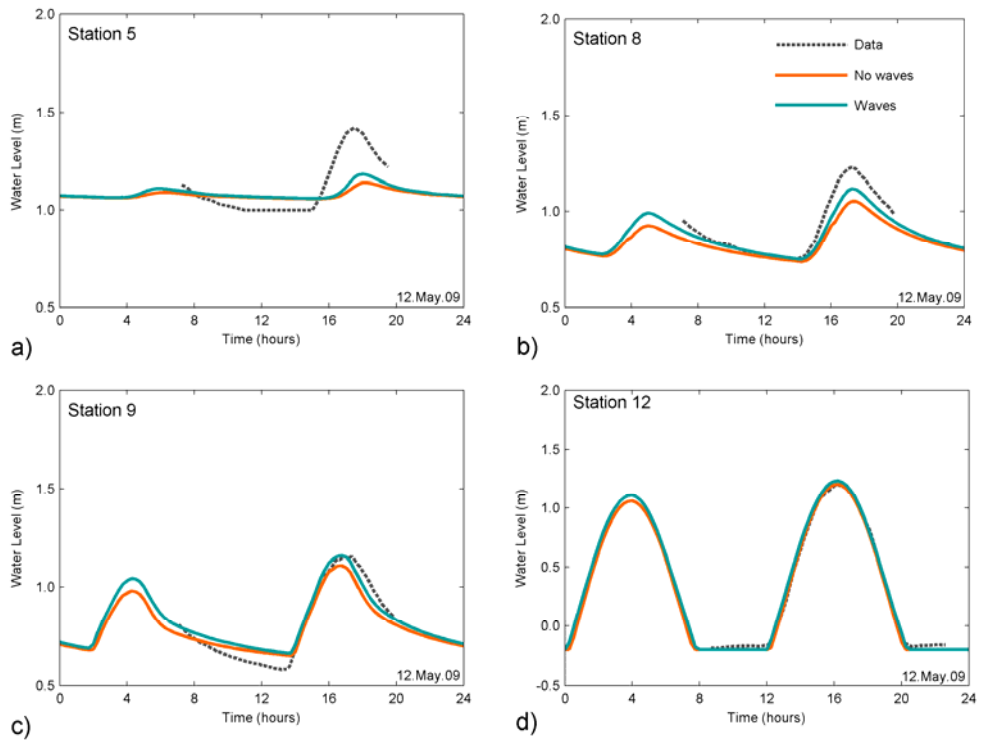


Figure 20 – Comparison between the elevation model results with and without the effect of waves.

Table 3 – RMS and Skill of the simulation results of water level and velocity for each station.

| | Station | RMS | | Skill | |
|-------------|---------|----------|-------|----------|-------|
| | | No Waves | Waves | No Waves | Waves |
| Water Level | 4 | 0.140 | 0.141 | 0.037 | 0.072 |
| | 5 | 0.129 | 0.115 | 0.404 | 0.581 |
| | 7 | 0.131 | 0.092 | 0.824 | 0.920 |
| | 8 | 0.090 | 0.057 | 0.887 | 0.958 |
| | 9 | 0.058 | 0.054 | 0.972 | 0.978 |
| | 11B | 0.031 | 0.040 | 0.999 | 0.999 |
| | 12 | 0.025 | 0.038 | 0.999 | 0.999 |
| Velocity | 9 | 0.513 | 0.501 | 0.528 | 0.544 |
| | 11B | 0.303 | 0.304 | 0.825 | 0.830 |

The results of the hydrodynamic component of MORSYS2D revealed the importance of the effect of waves inside of the system (Figure 20). The setup of the waves allows a further propagation of the tide, allowing a significant renewal of the water mass. The introduction of waves improved the values of RMS and skill performance especially in the mid-estuary stations (5, 7, 8 and 9).

From this calibration, the parameters with best results were afterwards used in the calibration of wave and sediment transport models.

5.4 LOW FREQUENCY WATER LEVELS

One important aspect in small coastal systems is the small variability in the water column. Considering the shallow depths in the inlet, the effect of atmospheric pressure in sea surface elevation should not be neglected. In chapter 3.2, the atmospheric pressure data from Sines Buoy was converted to values of water level fluctuations. Tests were performed to confirm the importance of the variability of the atmospheric pressure on the water depth, and its effect on the tidal propagation and the hydrodynamics in the Aljezur stream, by introducing this forcing along the boundary conditions of the circulation model (Figure 21).

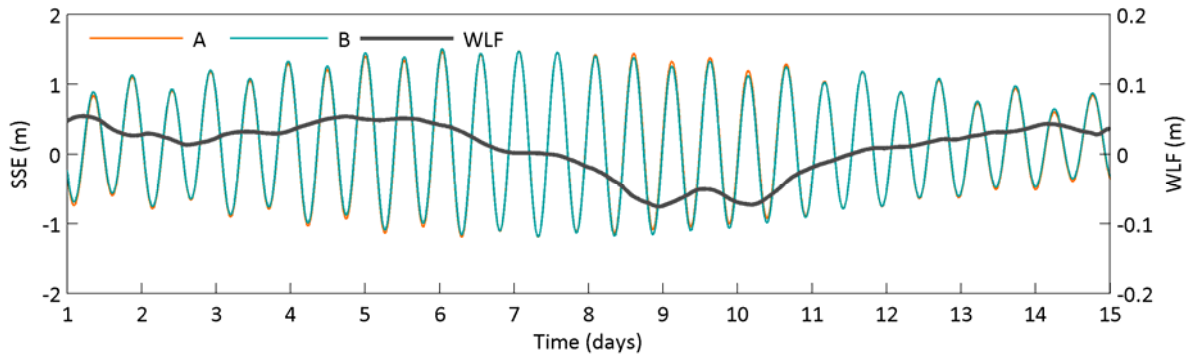


Figure 21 – Boundary condition for the simulation for the period May 1 – 15 2009, without (A) and with (B) the effect of the water level fluctuations (WLF).

Coupled wave-hydrodynamic simulations were performed for 15 days (starting on 1st May 2009), and the parameters were set equal from the previous calibrations of the circulation and wave models. Figure 22 shows the model results for simulations with and without the effect of atmospheric pressure between 9 and 13 of May 2009, for the stations 8 and 12, with special focus to the 10th day, when the water level fluctuations were large.

Figures 23 and 24 show the comparison between these model results and the data collected. For these simulations the RMS and Skill performance of the model were also calculated and are summarized in Table 4.

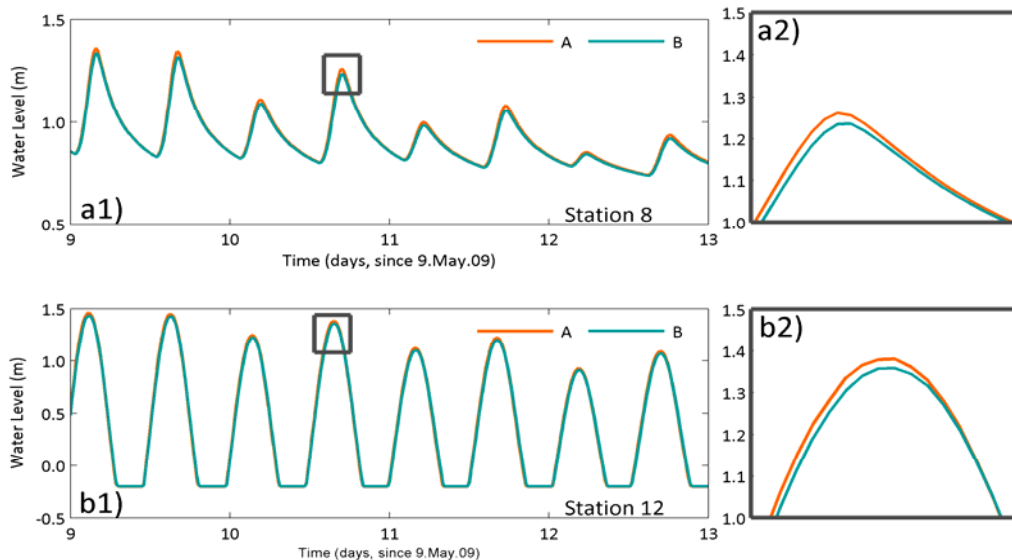


Figure 22 – Comparison between the water level data and the model results without (A) and with (B) the effect of the small water level fluctuations induced by the atmospheric pressure, for the period 9th – 13th May 2009, for the stations: a) 8 and b) 12.

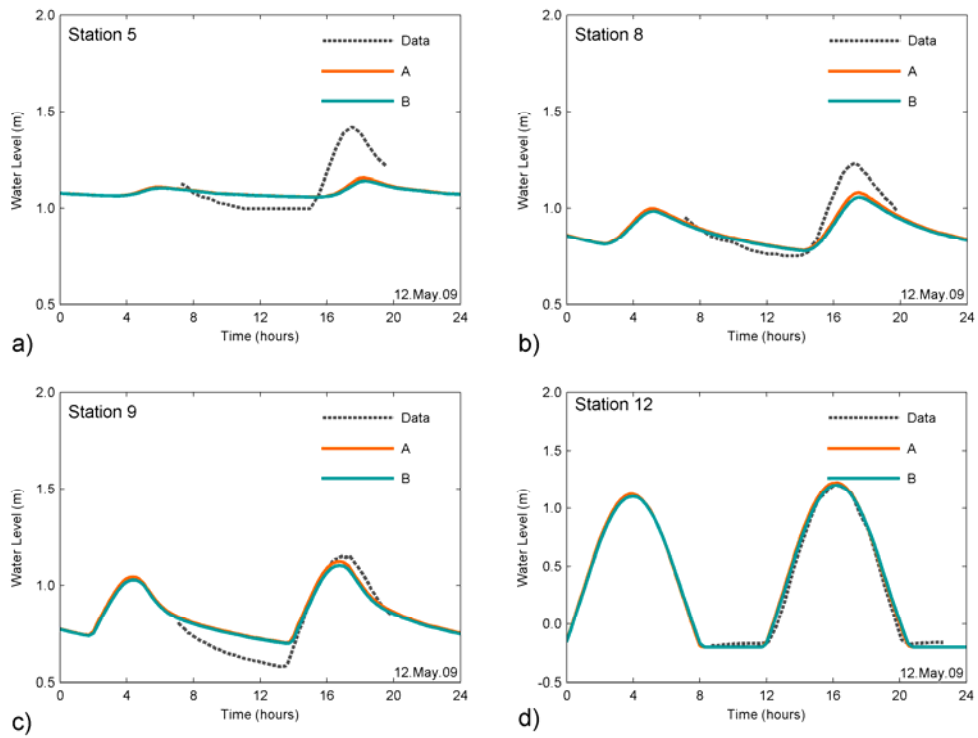


Figure 23 – Comparison between the water level data and the model results without (A) and with (B) the effect of the small water level fluctuations.

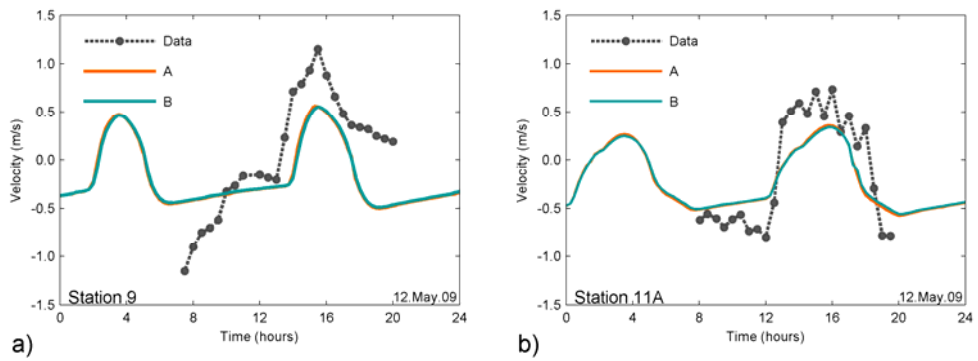


Figure 24 – Comparison between the velocity data and the model results without (A) and with (B) the effect of the small water level fluctuations.

Table 4 – Mean square error of the hydrodynamic simulation results of water level and velocities for each station.

| | Station | RMS | | Skill | |
|-------------|---------|--------|-------|--------|-------|
| | | No WLF | WLF | No WLF | WLF |
| Water Level | 4 | 0.135 | 0.135 | 0.054 | 0.041 |
| | 5 | 0.124 | 0.129 | 0.467 | 0.395 |
| | 7 | 0.106 | 0.121 | 0.873 | 0.829 |
| | 8 | 0.073 | 0.084 | 0.918 | 0.887 |
| | 9 | 0.080 | 0.079 | 0.943 | 0.943 |
| | 11B | 0.069 | 0.061 | 0.995 | 0.996 |
| | 12 | 0.056 | 0.047 | 0.997 | 0.998 |
| Velocity | 9 | 0.493 | 0.497 | 0.527 | 0.513 |
| | 11B | 0.305 | 0.311 | 0.820 | 0.807 |

Although the differences between simulation results are negligible for the campaign day (12th May 2009 – Figures 23 and 24), the results demonstrate how these small water level fluctuations forced in the boundary can affect the tidal propagation upstream (e.g., May 9, Figure 22). In conjunction with other factors, such as wind or waves setup, the global merging of the forcings has considerable impact in the total depth of the water column. Consequentially, this factor can lead to an alteration of the morphological behaviour and of the water renewal of the coastal system.

The addition of these small fluctuations improved slightly the values of RMS and performance skill. Although the improvement of the results for this particular period was smaller than expected, the effect of small variations in the total depth should not be neglected for simulations for long periods.

5.5 MORPHODYNAMICS

In spite of the limited skill of the model in the upper estuary, its ability to reproduce waves, water levels and currents in the tidal inlet area was considered adequate to study the morphodynamics in this region. From the previous calibrations, the major parameters were set to the following values: mean sea level – 2.15 m; drag coefficient – variable in space, $0.01 \text{ m}^{1/3}/\text{s}$ in the upper and mid estuary and $0.02 \text{ m}^{1/3}/\text{s}$ in the lower estuary; river flow – $0.3 \text{ m}^3/\text{s}$ (the value measured in May 2009); wave breaking coefficient – 0.8; wave dissipation rate – 0.5.

SAN2D simulations were performed with the same unstructured grid used in ELCIRC to avoid interpolations. The sediment grain size D_{50} was specified as spatially variable, from 0.26 to 0.34 mm, based on the collected sediment samples (Figure 10). Since the area of interest was the inlet region (lower estuary), bottom evolution was prevented in the mid- and upper-estuary, thereby reducing computational costs and avoid dealing with cohesive sediments. The time step was set to be adaptive from 2 min to 30 min, to avoiding spurious oscillations and reduce computational costs.

Sensitivity analyses to various physical and numerical approaches were performed. The tests included two alternative weak numerical filters (Fortunato and Oliveira, 2000), two sediment transport formulae (the Ackers and White formula (1973) adapted to waves by Van de Graff and van Overrem (1979) and the Soulsby - Van Rijn formula (Soulsby, 1997)) and two drag coefficient formulas (Soulsby and Manning). The Manning drag coefficient was used as either constant or variable in space. Figure 26 summarizes these sensitivity tests, which were performed for 15 days (starting on 1st May 2009) using as initial bathymetry the data from May 2009 (Figure 25).

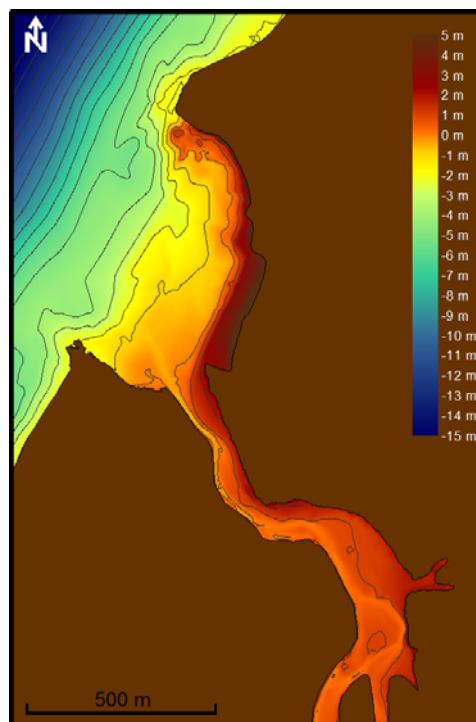


Figure 25 – Initial conditions of bathymetry. The bathymetry is colour-coded in meters, relative to mean sea level.

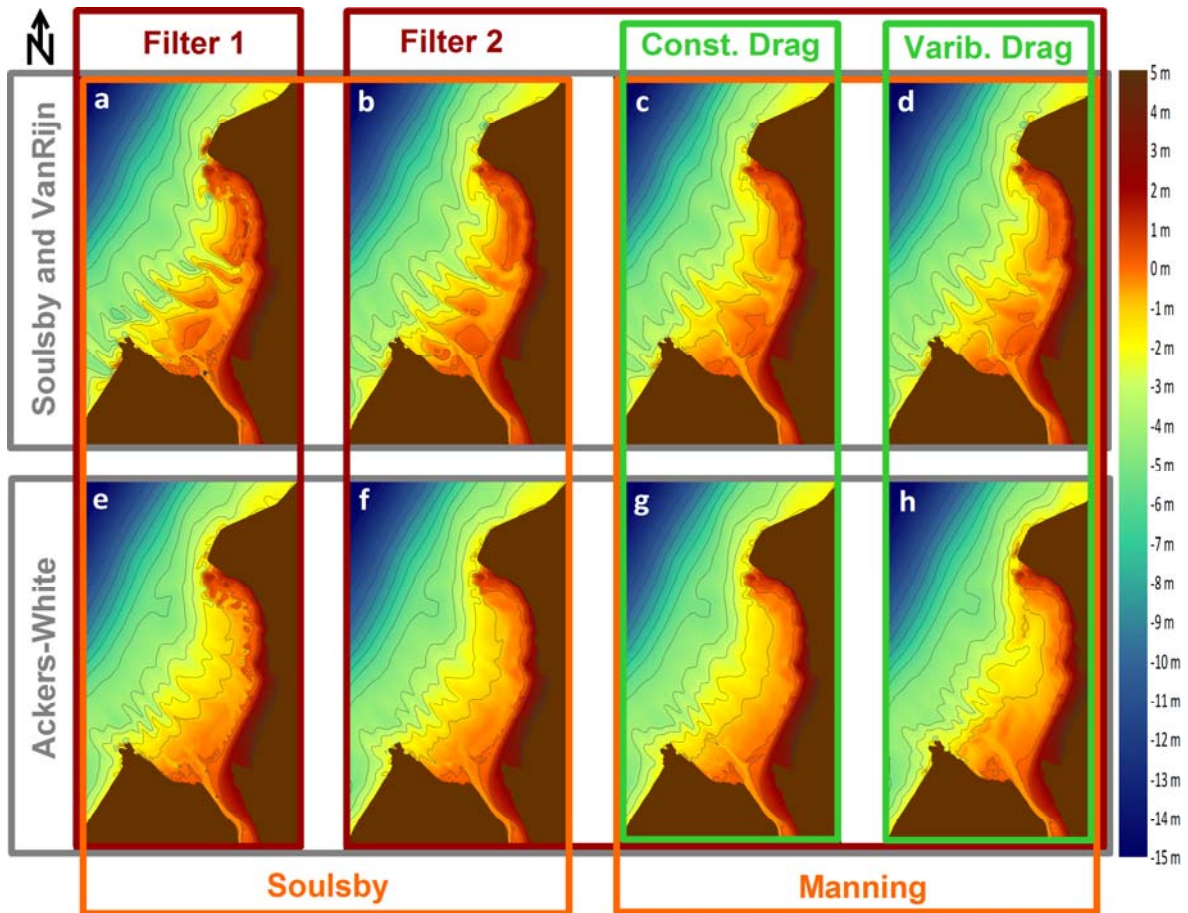


Figure 26 – Results from the sensitivity tests for the calibration of the sediment transport module. The bathymetry is colour-coded in meters, relative to mean sea level.

Several simulations led to unrealistic behaviours, including small-scale oscillations and cross-shore sand bathymetric features (Figure 26a, b and e). The options that led to the best results were retained: the sediment transport formula of Ackers and White and the variable Manning drag coefficient in space and filter 2 (Figure 26h). This filter damps $2\Delta x$ oscillations by eliminating local extrema (Fortunato and Oliveira, 2000).

Using these parameters, longer simulations were performed from May 10th till July 27th (78 days), a period that includes Campaign Two and the smaller coverage surveys (Figures 27 and 28).

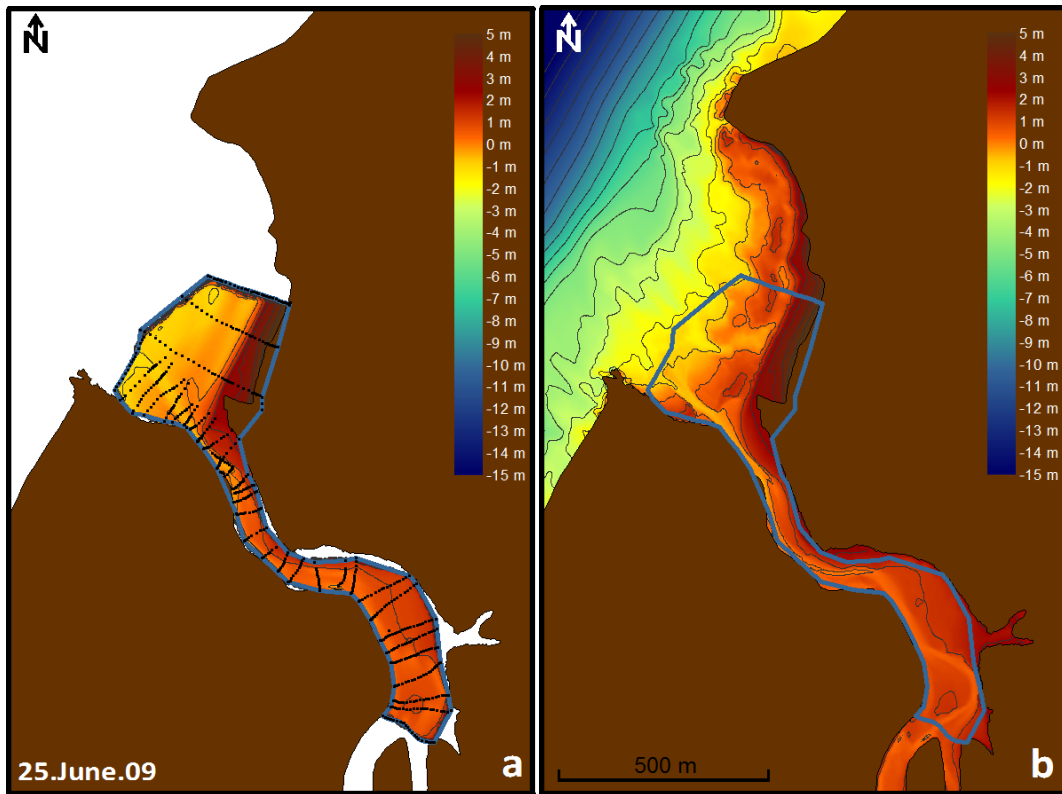


Figure 27 – Bathymetry at the lower-estuary, inlet and beach on June 25th 2009: a) data; b) model results. The bathymetry is colour-coded in meters, relative to mean sea level.

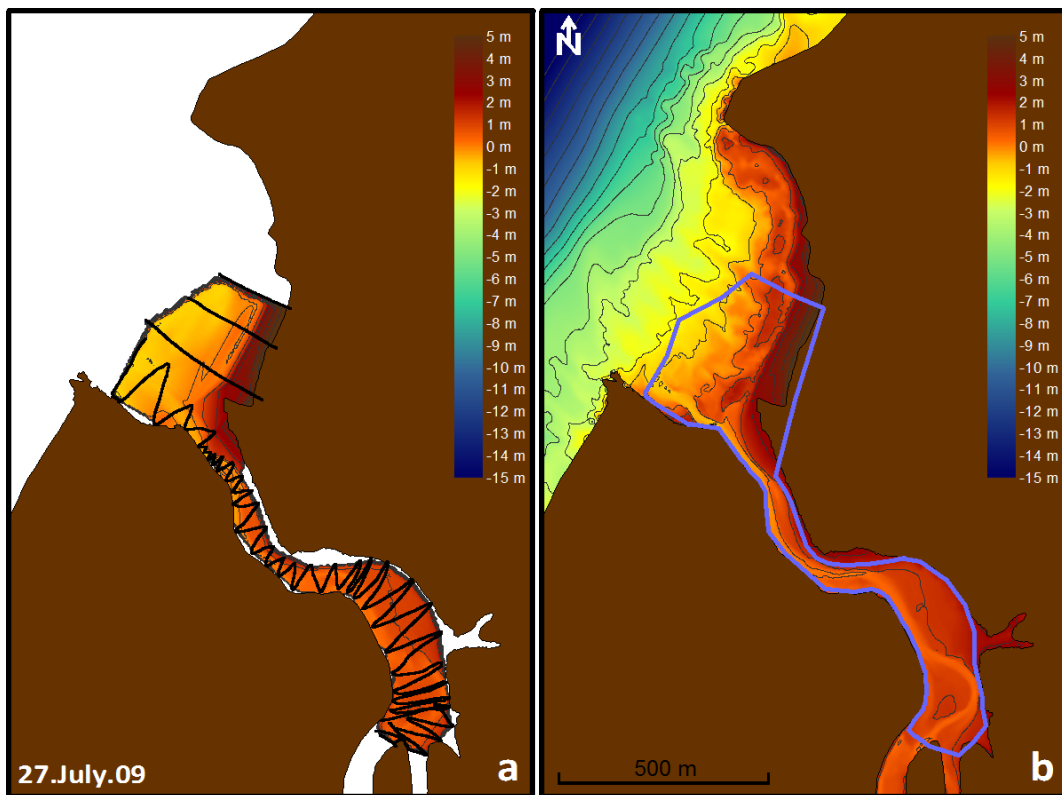


Figure 28 – Bathymetry at the lower-estuary, inlet and beach on July 27th 2009: a) data; b) model results. The bathymetry is colour-coded in meters, relative to mean sea level.

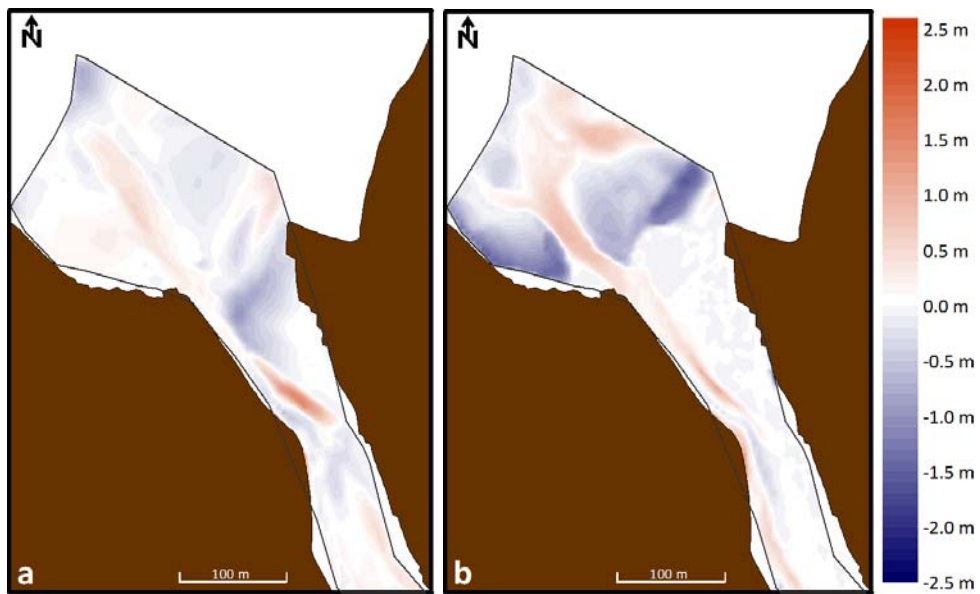


Figure 29 – Difference between: a) final data and initial conditions and b) simulations results and initial conditions on June 25th 2009. Positive (negative) values indicate erosion (accretion).

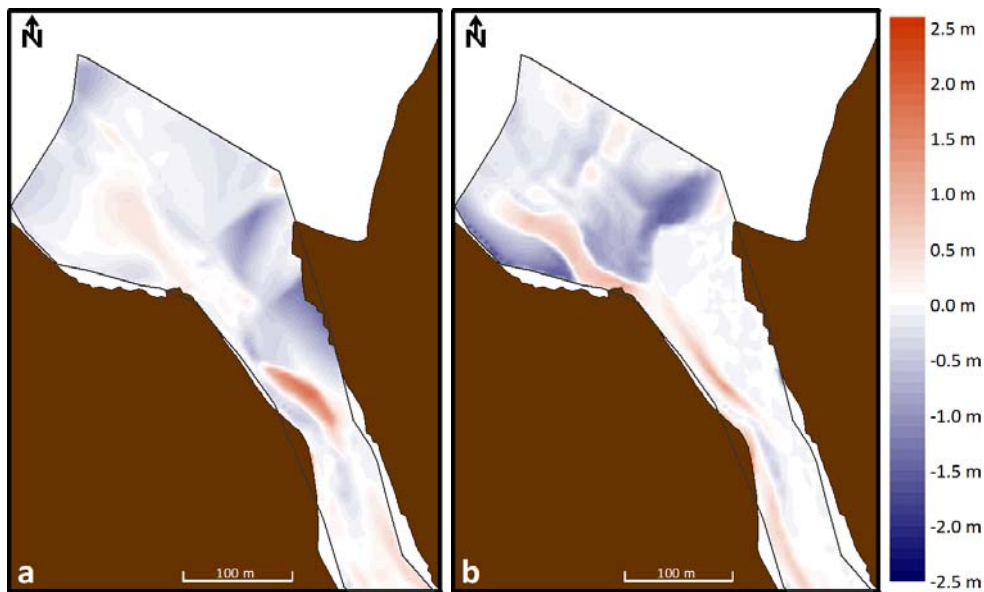


Figure 30 – Difference between: a) final data and initial conditions and b) simulations results and initial conditions on July 27th 2009. Positive (negative) values indicate erosion (accretion).

Results show that the model is able to qualitatively reproduce the behavior of the tidal inlet (Figure 29 and 30), including the deepening of the tidal inlet, the slight northward migration of the channel and the growth of the sand bank north of the inlet. Some trends are more pronounced in the model than in the data, suggesting that sediment transport is over predicted, but results appear adequate to investigate the qualitative effect of different forcings on the morphodynamic behavior of the inlet.

6. EXPLOITATION OF THE MODEL

The coastal system of Aljezur was monitored from 2008 till 2010. During this period, different configurations of the bathymetry were observed (Figure 27 and Figure 28), due to the variability of all forcings. This chapter aims at understanding the effect of some forcings on the behavior of the inlet through the exploitation of the morphodynamic model.

Two situations were studied: the influence of waves in the morphodynamic configuration of the Aljezur stream and the effect of very large river flow occurrences. In order to isolate these two aspects of the coastal system, all other forcings were kept unchanged. The model was forced by synthetic tides using one or two tidal constituents in order to simplify the interpretation of the results (M2 and M2S2, representing a spring and a neap tide, Figure 31) and simulations were performed for 15 days. The drag coefficient, time steps, artificial hotstart, computational grids and initial bathymetry were the ones defined in the calibration of MORSYS2D.

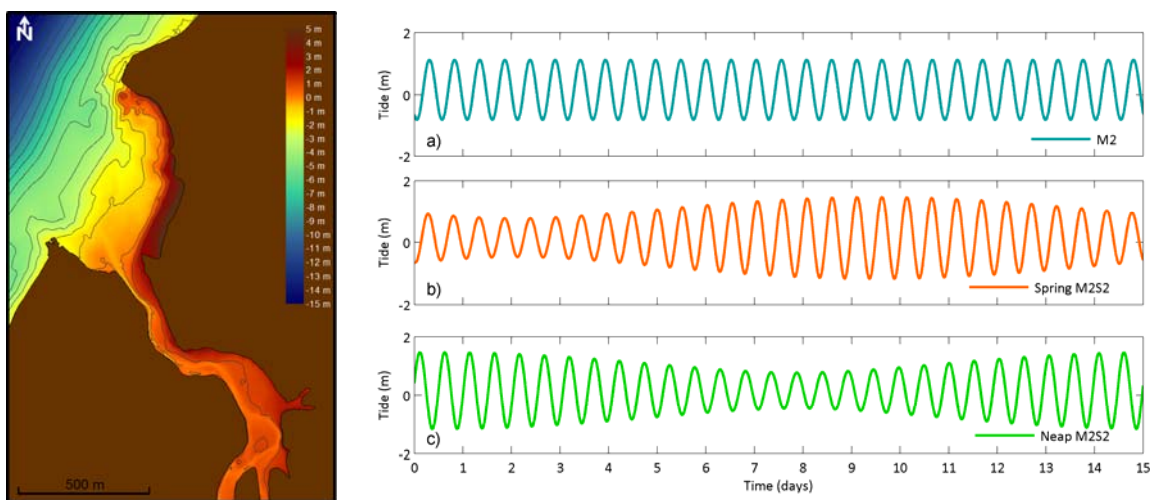


Figure 31 – Initial bathymetry (12th May 2009) and boundary conditions for the exploitation simulations: a) one tidal constituent and two tidal constituents for b) a spring tide and c) a neap tide.

6.1 WAVES

The wave climate of the southwest coast of Portugal is severe due to the influence of the North Atlantic winds and currents. Waves are predominantly from the NW/SW, with a mean significant wave height of 2 m. Tests were performed in order to understand the effect of waves on the morphodynamics of the Amoreira beach. Simulations were

performed with different significant wave heights, mean wave periods and directions, for the two synthetic tides. Table 5 summarizes the model setup for each simulation. Figures 32, 33 and 34 summarize the results after 15 days of simulation.

Table 5 – Characteristics of the synthetic numerical tests for the wave forcing simulations. The color lines correspond to the figures below: Figure 32 (—), Figure 33 (—) and Figure 34(—).

| Tide | M2 | | | | | | | | | M2S2 | | |
|-----------|----|---|----|----|---|----|----|---|----|------|---|----|
| T (s) | 5 | | | 10 | | | 15 | | | 10 | | |
| Direction | NW | W | SW | NW | W | SW | NW | W | SW | NW | W | SW |
| Hs (m) | | | | | | | | | | | | |
| 1 | | | | a | b | c | | | | | | |
| 2 | a | b | c | d | e | f | g | h | i | a | b | c |
| 3 | | | | g | h | i | | | | | | |

Results show that the erosion of the Amoreira beach increases with the wave energy. Indeed, both an increase in wave height (Figure 32) and period (Figure 33) push the isobaths further offshore. In contrast, the wave direction has a profound effect on the configuration of the channels (Figure 32). NW waves push the channel northward, close to the cliffs, whereas W and SW waves push the channel southward. SW waves also create a secondary channel and a large bank that follows the beach northward. A channel of this type has been observed both in the spring and summer 2010 (Figure 9). Finally, the comparison between Figures 33 and 34 suggests that the morphodynamic changes in the Amoreira beach due to the effect of waves are fairly insensitive to the effect of tides.

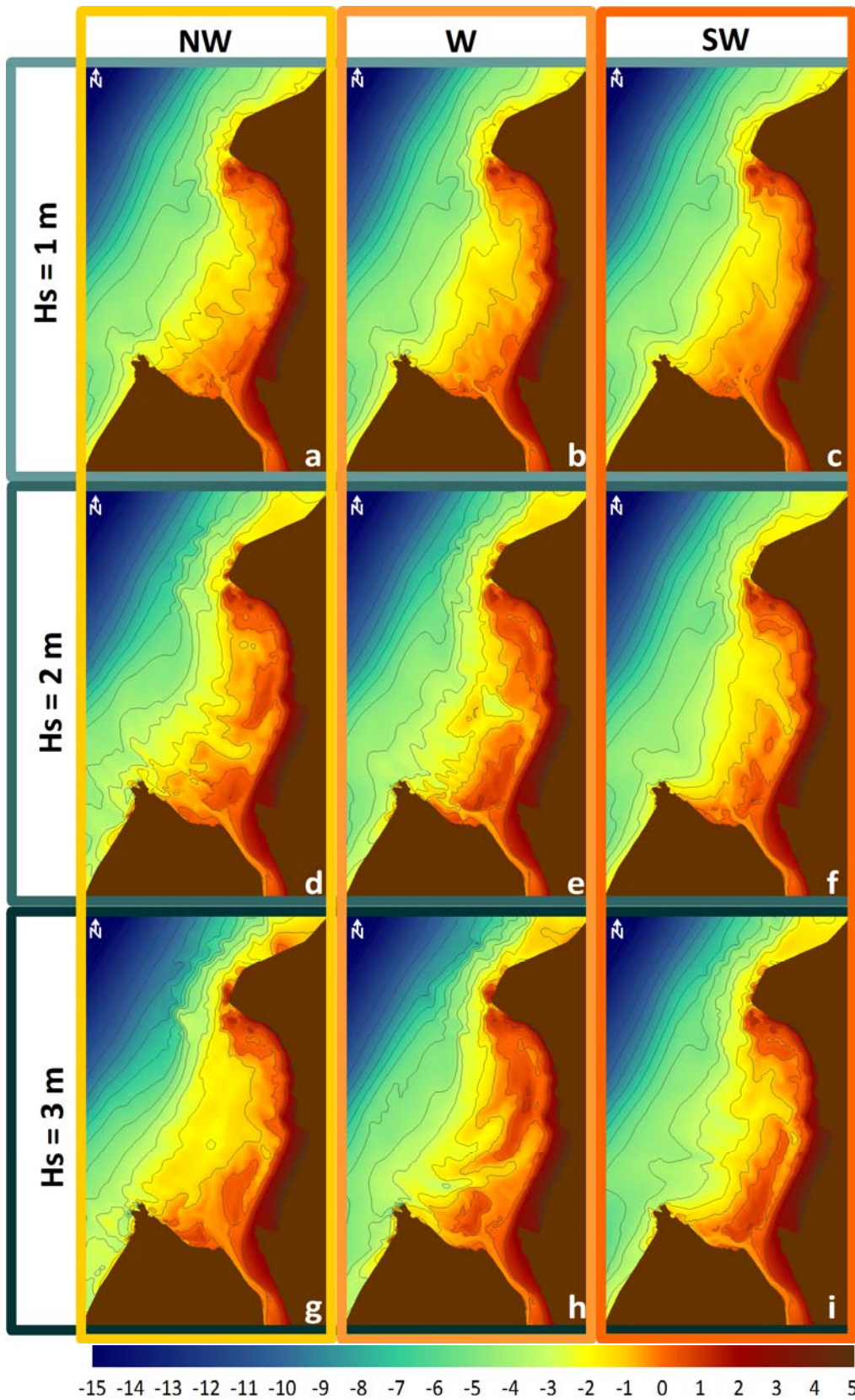


Figure 32 – Effect of the significant wave height (1, 2 and 3 m) and the wave direction (NW, W and SW) on the morphology of the Amoreira beach. See Table 5 for details.

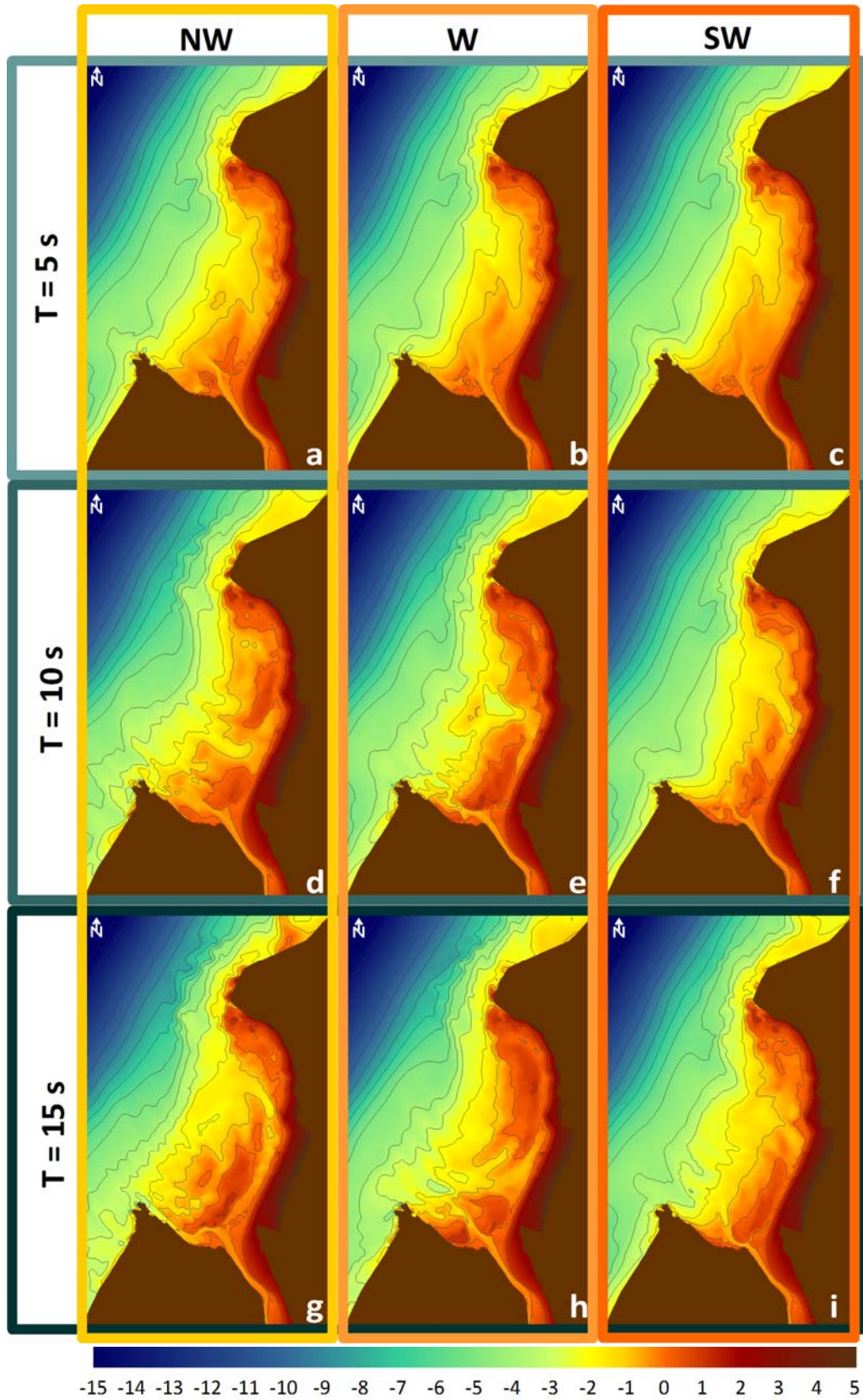


Figure 33 – Effect of the wave period (5, 10 and 15 s) and the wave direction (NW, W and SW) on the morphology of the Amoreira beach (see Table 5 for details).

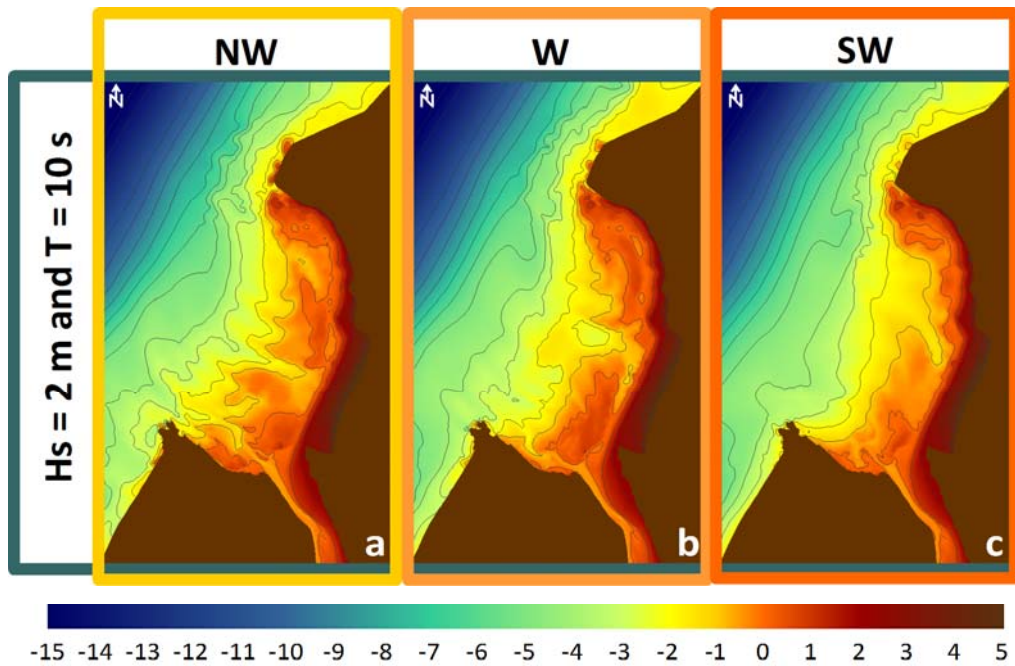


Figure 34 – Wave exploration results for a constant significant wave height ($H_s = 2$ m), constant wave period ($T = 10$ s) and with a variation of the wave direction (NW, W and SW), for a synthetic tide M2+S2.

6.2 HIGH RIVER FLOWS

The second set of exploitation tests aimed at understanding the response and recovery of the system under high river flows resulting from large precipitation events. This set of tests also aims at distinguishing when the river flow is able to overlap the effect of tidal currents in the morphodynamics variability of the inlet, through the variation of the maximum and duration of the peak flows.

Several tests were performed with the two synthetic tides: M2 and M2S2. For the M2, four peak flows were simulated with maximum flow of 1, 5, 10 and 15 m^3/s during different durations of 5, 10 and 15 hours. Simulations were performed for a period of 15 days. The river flow was constant (0.3 m^3/s) in the beginning of the simulation and the peak flows started at the 5th day of simulation. For the M2+S2, these tests target the analysis of the periods of spring and neap tides. A peak flow of 5 m^3/s during 10 hours was set to begin during these tides, at the 9th day of simulation. Wave conditions were set to be constant, with a direction from NW, a significant wave height of 2 m and a wave period of 10 s, representing a typical situation in the SW Portuguese coast.

Figure 35 shows the results for the different maxima for the peak river flow for the 7th day, and Figure 36 shows the results for the peak flow of 5 m³/s with different durations, for the 7th, 10th and 15th day of simulation for a synthetic tide M2. Figure 37 shows the simulations for the synthetic tide M2+S2.

Along with the visual analysis of the bathymetry, a cross section analysis was performed to measure the variability of the channel under these different conditions. Figures 38 and 39 summarize this analysis.

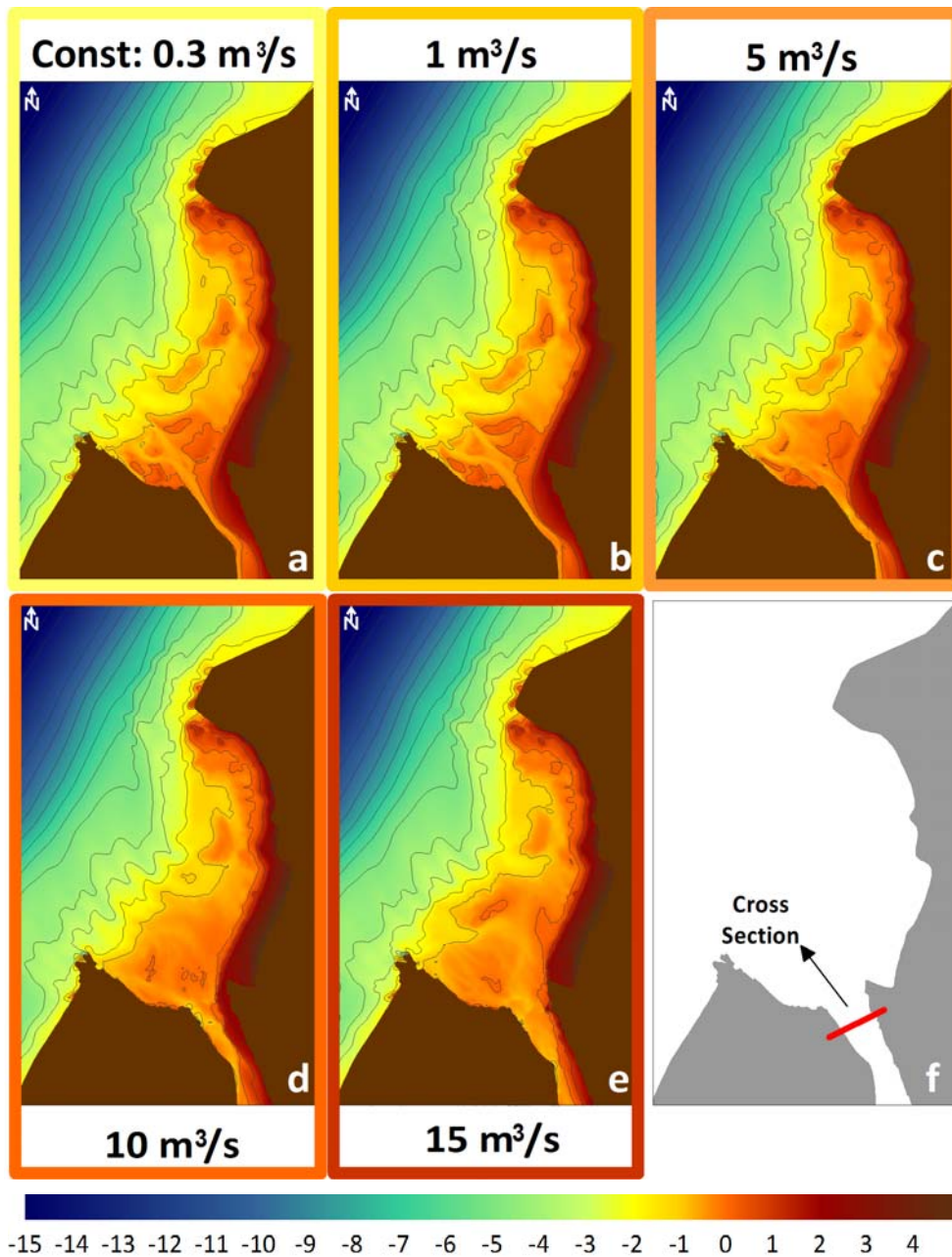


Figure 35 – Simulation results for the 7th day of simulation of: a) constant river flow of 0.3 m³/s and to maximum peak flow of b) 1 m³/s, c) 5 m³/s, d) 10 m³/s and e) 15 m³/s during 10 h; and f) correspond to the location of the cross section analysis. The results correspond to the simulations with a synthetic tide M2.

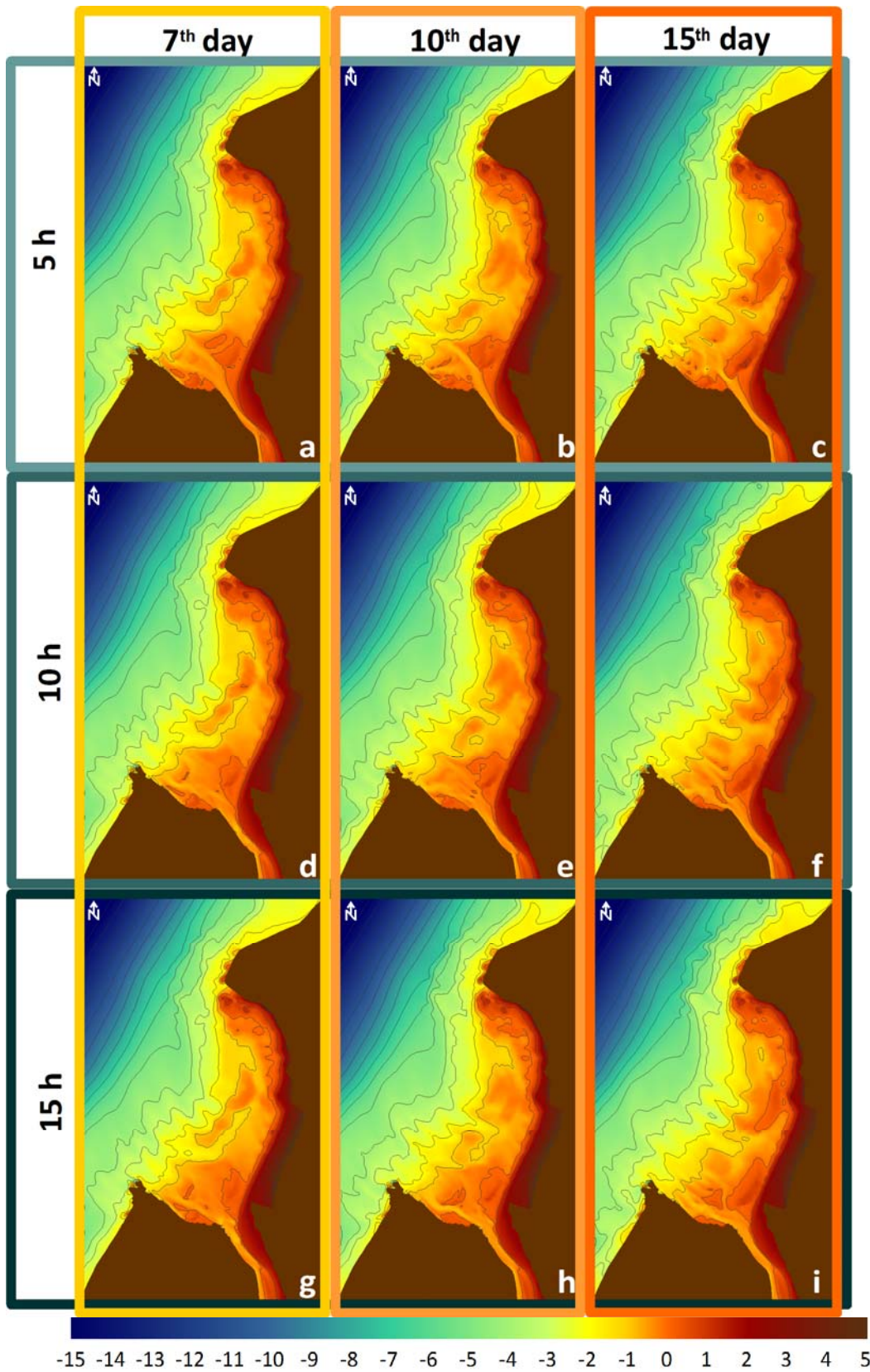


Figure 36 – Results to the peak flow of $5 \text{ m}^3/\text{s}$, during 5 (a, b and c), 10 (d, e and f) and 15 h (g, h and i). The results correspond to the 7, 10 and 15 days of simulation for a synthetic tide M2.

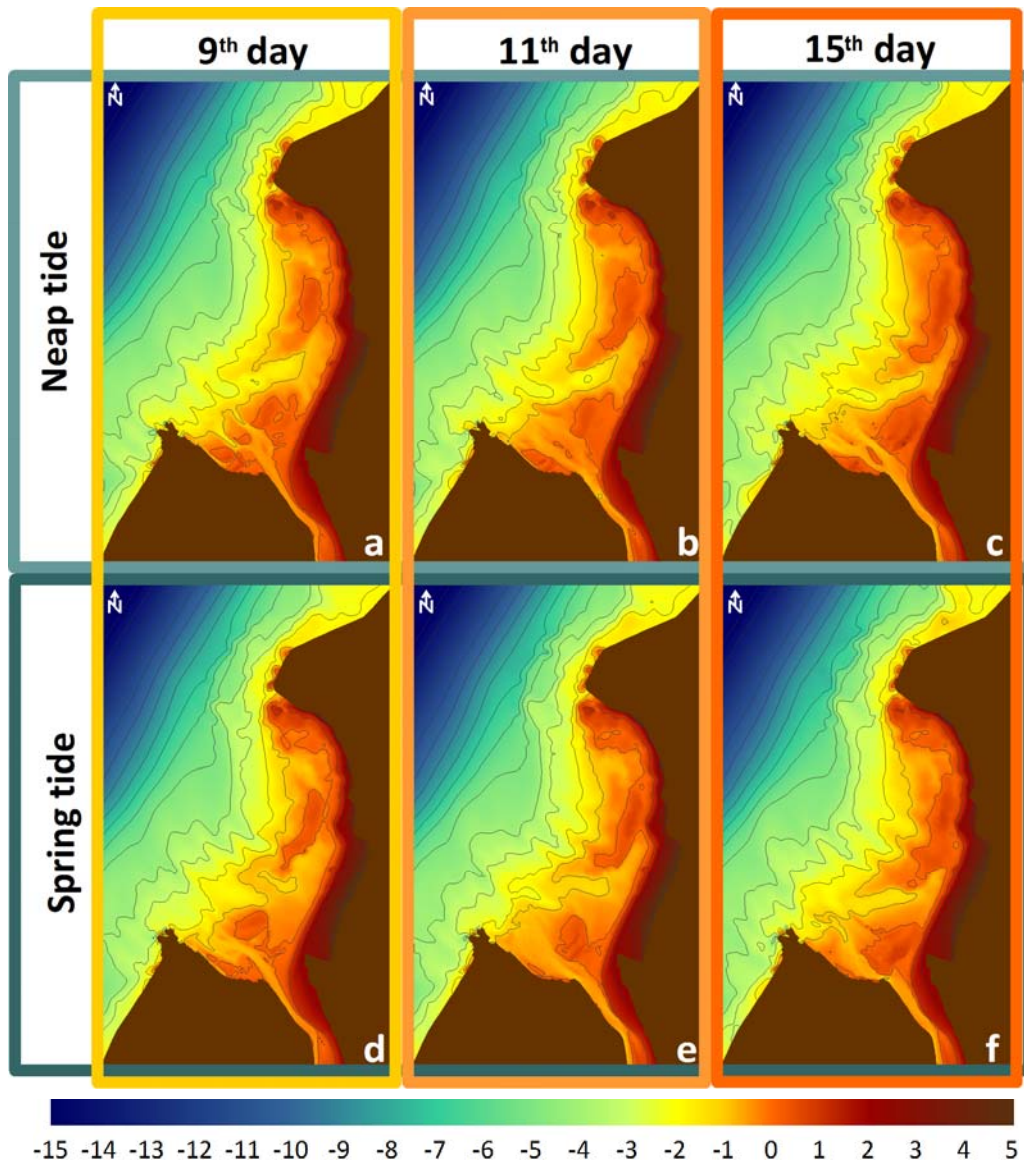


Figure 37 – Results to the peak flow of $5 \text{ m}^3/\text{s}$, during 10 hours. The results correspond to the 9, 11 and 15 days of simulation for a synthetic tide M2+S2. Neap tide (a, b, c) and spring tide: (d, e, f).

The temporal evolution of the inlet after the maximum flow shows that the increase of the flow affects mainly the region near the inlet, along and up to the end of the cliff to the south (Figures 35 and 36).

In the simulations with the synthetic tide M2, results show a stronger erosion of the inlet region with the increase of the duration of the peak flow but especially with the increase of the maximum peak. From Figure 36, the results show the recovery of the inlet with the growth of sand banks 5 days after the event, suggesting that although the impressive momentum effect, the tidal currents and waves tend to eliminate the morphological changes produced by these type of events after a few days.

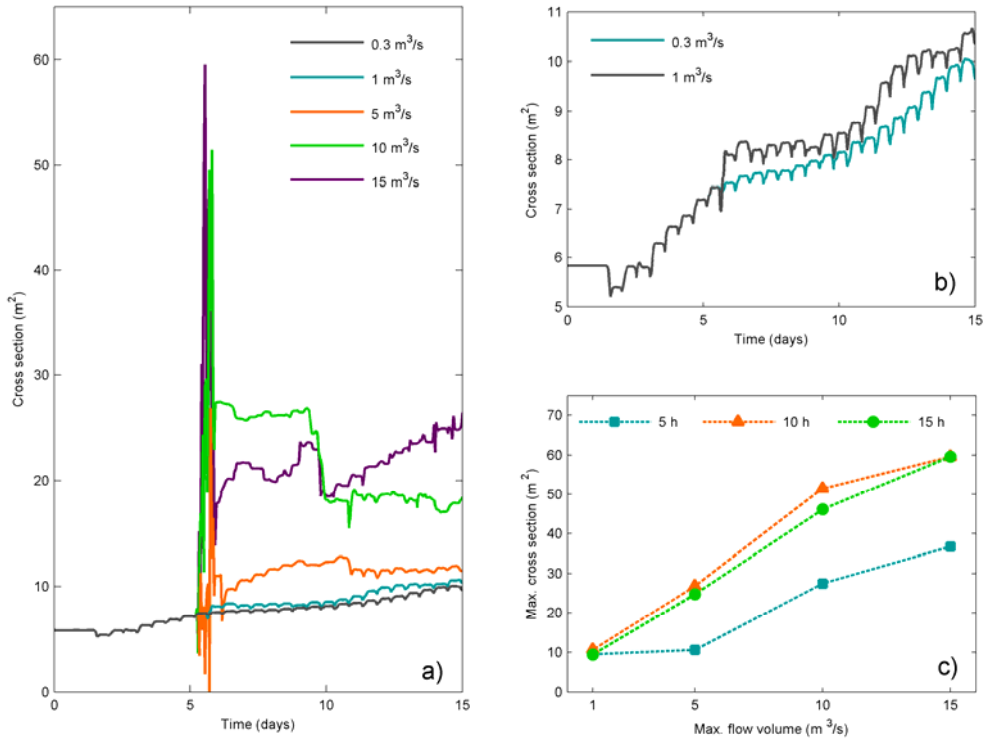


Figure 38 – Analyze of the cross section at the inlet: a) evolution along the 15 days simulation for the different maximum peaks and a duration of 10 h, b) detail for the evolution with a constant river flow and a maximum peak of 1 m³/s and c) correlation between maximum flow volume and cross section for the different durations.

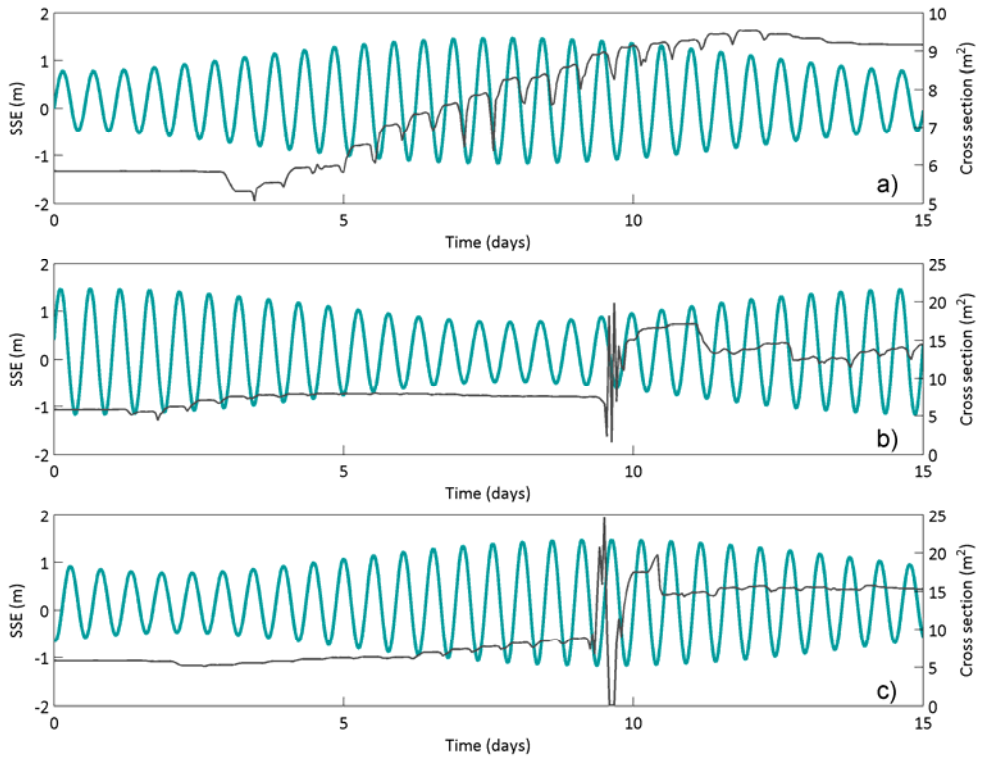


Figure 39 – Cross sections results to each M2S2 versus river flow: a) a constant river flow of 0.3 m³/s during all simulation, and a peak flow of 5 m³/s during 10 hours, at the 9th day of simulation during a b) neap and c) spring tide

The inlet cross section tends to increase gradually during the simulation, although with tidal fluctuations. A small peak flow of 1 m³/s further increases the cross-section, but does not affect the growth trend (Figure 38 – b).

With a longer and larger peak flow, the cross section tends to suffer a dramatic change for a short period but is able to re-establish the previous values after a few days. Also, the analysis shows that the maximum cross section increases with the duration and maximum peak flow volume (Figure 38 – c).

From the simulations with the two tidal constituents, representing a neap tide and a spring tide, results show the combination of both effects. Morphodynamic changes are more intense during the spring tide, keeping the same position of the channel at the beach. For the neap tide the channel tends to shift southward towards the cliff. During the neap tide, the erosion is smaller than in the spring tide.

The cross section analysis of these simulations show that the cross section tends to increase with the increase of the tidal amplitude (Figure 39 –a). When the peak flow events occur, the inlet suffers erosion, which is amplified with spring tides.

From these exploitation scenarios the model demonstrated how important this type of events are to the morphologic changes in the inlet, keeping the stream connected to the sea.

7. DISCUSSION AND CONCLUSIONS

The main goal of this study was to contribute to the understanding of the morphologic variability of the coastal system of the Aljezur stream, through the application, calibration and validation of MORSYS2D. Throughout this work, the simulation of the morphodynamics of this coastal system proved to be a challenging task: many forcings must be taken into consideration (e.g., tides, waves, river flow, atmospheric pressure), the bathymetric data were scarce in many areas and model documentation was poor.

This work was divided into three major steps: 1) extensive field campaigns were conducted to provide the necessary data; 2) the morphodynamic model MORSYS2D was implemented in the system, then calibrated and validated with the field data collected in the campaigns; 3) the model was then used to investigate selected aspects of the morphodynamic behavior of the Aljezur inlet.

The field campaigns provided the data required to better understand and characterize the coastal system and its variability. The bathymetric data and the Amoreira beach photos, acquired every few months, reveal the morphological characteristics during the two years of monitoring. The high variability in a single spring tide cycle was surprising, revealing the vulnerability of the stream to potential disturbances.

During field campaigns, a few obstacles were presented by the system. Station locations were limited to the regions where the dense vegetation along the stream allowed the access to the stream. Also, the dense vegetation combined with the type of sediments (mostly regions with sludge), the shallow depth and the narrow width of the stream, led to a poor bathymetry acquisition in the mid and upper estuary. In the lower estuary and beach, the need to measure the bathymetry only at low tide also led to a sparse acquisition of bathymetry during the small surveys.

The processing and analysis of the data revealed some inconsistencies, and part of the data had to be discarded. However, in the end, the data was adequate, quantitatively and qualitatively, to characterize the coastal system.

The amount of data with good quality was essential to perform a realistic implementation of the morphodynamic model. Water level, velocity and wave data

collected along the stream and at the beach were used to calibrate the hydrodynamic component, and the several sets of bathymetry allowed the final calibration of the morphodynamic component.

MORSYS2D was an essential tool for this study. Several model runs were performed for each step to calibrate each component of MORSYS2D. The final results show in general a good performance, although the accuracy of the hydrodynamic model progressively degrades upstream. The RMS errors range from 3% to 10% of the local amplitude, and skill values higher than 0.89 were reached for the stations in the lower estuary (stations 8 to 12) for elevations. The calibration for velocities was less successful. The RMS errors were about 30% to the station 11B and 50% to station 9, and skill values higher than 0.8 and 0.5 to station 11B and 9, respectively. The calibration procedure revealed the importance of including waves (and, to a smaller extent, atmospheric pressure fluctuations) to accurately propagate tides upstream.

Differences may be due to the complexity of the coastal system, where the shape and the morphodynamics of the inlet, strongly affect the tidal propagation. Also, small inconsistencies in the initial bathymetry and data may increase the error.

Relatively to the morphodynamic component, the model was able to reproduce the main characteristics observed during the smaller campaigns, such as the deepening of the tidal inlet, the slight northward migration of the channel and the growth of the sand bank north of the inlet.

Computational costs were an important limitation of the model. In spite of the significant computational resources available (a 264-node cluster), and the improvements in the model efficiency implemented in parallel with this work (Bruneau *et al.*; 2010, Costa *et al.*, 2010), the simulations were performed almost in real time due to the dimensions of the computational grid (about 40000 nodes).

After the accuracy of the model application was established, MORSYS2D was used to understand the behavior of the system under different forcings. In particular, it was examined the impact of wave characteristics on the beach behavior, and the response of the system to high peak river flows.

The morphodynamic variability of the beach is dominated mostly by the waves, which shifting (northward or southward) the channel depending on their directions. The amplitude of the tide affects how far upriver and onshore the waves can reach.

The river flow dominates the morphodynamics of the inlet region when peak flows occur, overlapping the tidal currents and waves effect. During the dry season, when river flow is almost inexistent, the cross section of the inlet tends to increase with the tidal amplitude. When the peak flow events occur, the inlet is eroded, a behavior that is amplified on spring tides. High river discharges thus contribute to keeping the stream connected to the sea.

This study brought a new understanding of the system and its variability. The exploitation of MORSYS2D offers the possibility to answer questions about the morphodynamics of this coastal system.

The exploitation tests performed in chapter 6 provided some insight into the behavior of the system. However, other exploitation simulations should be performed to answer further questions on the system behavior. For instance, the salt marsh region has been severely reduced by the construction of the aquaculture ponds in the 1990's. The change in the surface area of the salt marsh is likely to affect the tidal prism, and ultimately the morphodynamics of the inlet, as has been shown in other systems (e.g., Picado *et al.*, 2008). MORSYS2D could be used to quantify these changes. Also, storm events are likely to have a profound effect on the inlet. Again, MORSYS2D could be used to assess the extent of these changes and the time needed for the beach to recover. The effect of wind-generated currents and setup could be investigated using the model. Finally, it would be interesting to simulate past events that led to the closure of the system to understand which processes and forcings were the most relevant.

8. REFERENCES

- Ackers, P., White, W.R., 1973. Sediment transport: new approach and analysis. *Journal of Hydraulics Division* 99 (1), 2041–2060.
- Almeida *et al.*, 2000. Plano de Bacia Hidrográfica das Ribeiras do Algarve, 1ª fase, Volume III, Ministério do Ambiente e do Ordenamento do Território.
- Bertin, X., Fortunato, A.B., Oliveira, A., 2009a. Morphodynamic modeling of the Ancão Inlet, South Portugal, *Journal of Coastal Research*, SI56: 10-14.
- Bertin, X., Oliveira, A., Fortunato, A.B., 2009b. Simulating morphodynamics with unstructured grids: description and validation of a modeling system for coastal applications. *Ocean Modelling*, 28/1-3: 75-87.
- Bertin, X., Fortunato, A.B., Oliveira, A., 2009c. A modeling-based analysis of processes driving wave-dominated inlets. *Continental Shelf Research*, 29/5-6: 819-834.
- Bertin, X., Fortunato, A.B. and Roelvink, D., 2010. Morphodynamic Modelling of Tidal Inlets and Embayments. In: *Geomatic Solutions for Coastal Environments*. Editors: M.Maanan and M. Robin, Nova Science Publishers Inc., pp.197-213, ISBN 978-1-61668-140-1.
- Booij, N., Ris, R., Holthuijsen, L., 1999. A third-generation wave model for coastal regions. 1. Model description and validation. *Journal of Geophysical Research* 104 (7), 649–666.
- Bruneau, N., Fortunato, A.B., Oliveira, A., Bertin, X., Costa, M., Dodet, G., 2010. Towards long-term simulations of tidal inlets: performance analysis and application of a partially parallelized morphodynamic modeling system, *Computational Methods in Water Resources XVIII*, in press.
- Cayocca, F., 2001. Long-term morphological modeling of a tidal inlet: the Arcachon Basin, France. *Coastal Engineering*, 42: 115–142.
- Costa, A.M, Cancela da Fonseca, L., Bernardo, J.M., Moita, I., 1987. Sistemas Lagunares de Odeceixe, Aljezur e Carrapateira (SW de Portugal): algumas causas e implicações do seu assoreamento. *Actas do I Congresso Nacional de Áreas Protegidas*, pp 393-399.
- Costa, A.M, Bernardo, J.M., Cancela da Fonseca, L., 1988. Sistemas Lagunares de Odeceixe, Aljezur e Carrapateira (SW de Portugal): Confinamento e produtividade. *Actas do 5º congresso do Algarve*.
- Costa, A.M, 1993. Bio-ecologia de *Cardium edule* (LINEU, 1767) e de *Cardium glaucum* (Bruguíere 1789) nos estuários de Odeceixe e de Aljezur (Sudoeste de Portugal). *Doctoral thesis, Universidade de Évora, Portugal*, pp 253
- Costa, M., Bruneau, N., Oliveira, A., Fortunato, A.B., 2010. Optimizing I/O in a morphodynamic model, *Ibergrid 2010*, in press.
- Dias J.M., Sousa M., Bertin X., Fortunato A., Oliveira A., 2009. Numerical modeling of the impact of the Ancão Inlet relocation (Ria Formosa, Portugal). *Environmental Modelling & Software*. 24, 711-725.

- Dodet G., Bertin, X. and Taborda, R. 2010. Wave climate variability in the North-East Atlantic Ocean over the last six decades. *Ocean Modeling*, 31 (3-4), 120-131.
- Fidalgo e Costa, P., Brotas, V., Cancela da Fonseca, L., 2002. Physical characterization and Microphytobenthos biomass of estuarine and lagoon environments of the SW coast of Portugal. *Limnetica*, 21:69-79.
- Fidalgo e Costa, P., 2003. The oogenic cycle of *Nereis diversicolor* (O.F. Müller, 1776) (Annelida: Polychaeta) in shallow water environments in southwestern Portugal. *Bol. Inst. Esp. Oceanogr.* 19 (1-4), 17-29.
- Fortunato, A.B. and Oliveira, A., 2000. On the representation of bathymetry by unstructured grids. *Computational Methods in Water Resources XIII*, Balkema, Vol. 2, pp. 889-896.
- Fortunato, A.B., Pinto, L., Oliveira, A., Ferreira, J.S., 2002. Tidally generated shelf waves off the Western Iberian Coast. *Continental Shelf Research* 22 (14), 1935–1950.
- Fortunato, A.B., Oliveira, A., 2004. A modeling system for tidally driven long-term morphodynamics, *J. Hydraulic Research*, 42/4: 426-434.
- Fortunato, A.B., 2007a. Accuracy of sediment flux computations in tidally-driven simulations. *J. Waterways, Ports, Coastal and Ocean Engineering*, 133/5: 377-380.
- Fortunato, A.B., Oliveira, A., 2007b. Improving the stability of a morphodynamic modeling system, *J. Coastal Research*, SI50: 486-490.
- Fortunato, A.B., Oliveira, A., 2007c. Case study: promoting the stability of the Óbidos lagoon inlet, *J. Hydraulic Engineering*, 133(7): 816-824.
- Fortunato, A.B., Bruneau, N., Azevedo, A., Araújo, M.A.V.C., Oliveira, A., 2010. Automatic improvement of unstructured grids for coastal simulations, *International Coastal Symposium – ICS 2011* (submitted)
- Freire, P., Taborda, R., Bertin, X., Fortunato, A.B., Andrade, C., Oliveira, A., Antunes, C., Guerreiro, M., Freitas, C.M., Nahon, A., Silva, A.M., Rodrigues, M., 2010a. Medium-term morphodynamic evolution of a small coastal, *International Coastal Symposium – ICS 2011* (submitted).
- Freire, P., 2010b. Relatório 4: Relatório técnico da campanha MADyCOS 03 (07/09/2009 a 09/09/2009). Relatório 328/10 – NEC/NTI/NPE/NES, pp 35.
- Gama-Pereira, C., 2005. Dinâmica de sistemas sedimentares do litoral ocidental português a sul do Cabo Espichel. PhD thesis, Universidade de Évora, Portugal.
- Kirby, J. T. and Dalrymple, R. A., 1994. Combined Refraction/Diffraction Model REF/DIF 1, Version 2.5. Documentation and User's Manual", Research Report No. CACR-94-22, Center for Applied Coastal Research, Department of Civil Engineering, University of Delaware, Newark.
- Luetlich, R.A., Westerink, J.J. and Sheffner, N.W., 1991. ADCIRC: An Advanced Three-Dimensional Model for Shelves, Coasts and Estuaries. Report 1: Theory and Methodology of ADCIRC-2DDI and ADCIRC-3DL, Department of the Army, US Army Corps of Engineers.

- Magalhães, F., Cancela da Fonseca, L., Bernardo, J.M., Costa, A.M., Moita, I., Franco, J.E., Duarte, P., 1987. Physical characterization of Odeceixe, Aljezur and Carrapateira lagunary systems (SW Portugal). *Limnetica*, 3(2): 211-218, 1987.
- Nahon, A., Bertin, X., Fortunato, A.B., Oliveira, A., 2009. A modeling-based assessment of tidal inlet classification. Colloque SHF: "Morphodynamique et gestion des sédiments dans les estuaires, les baies et les deltas", CD-ROM, 13pp.
- Nahon, A., Fortunato, A.B., Bertin, X., Oliveira, A., Freitas, C., Pirea, A.R., Andrade, C., 2010. Modelação morfodinâmica de uma barra de maré efémera: Lagoa de Santo André, Portugal. MEC – 2011, Portugal (submitted).
- Oliveira, A., Fortunato, A.B., Rodrigues, M., Azevedo, A., 2007. Integration of physical and water quality models, *Houille Blanche*, 4: 40-46.
- Oliveira, A., 2009. Relatório 1: Relatório técnico da campanha MADyCOS 00 (05/05/2008 a 07/05/2008). Relatório 09 – NEC/NTI/NPE/NES, pp 49.
- Oliveira, A., 2010a. Relatório 2: Relatório técnico da campanha MADyCOS 01 (10/09/2008 a 12/09/2008). Relatório 15/09 – NEC/NTI/NPE/NES, pp 48.
- Oliveira, A., 2010c. Relatório 3: Relatório técnico da campanha MADyCOS 02 (11/05/2009 a 13/05/2009) Relatório 123/10 – NEC/NTI/NPE/NES, pp 37.
- Oliveira, A., Fortunato, A.B., Guerreiro, M., Bertin, X., Bruneau, N., Rodrigues, M., Tabora, R., Andrade, C., Silva, A., Antunes, C., Freire, P., Pedro, L., Dodet, G., Loureiro, C., Mendes, A., 2010c. Effect of inlet morphology and wave action on pollutant pathways and sediment dynamics in a coastal stream, ICM11 – 11th Estuarine and Coastal Modeling, ASCE, Spauling *et al* (eds).
- Picado, A.T.S., 2008. Degradation of the salt pans in Ria de Aveiro: an Hydrodynamical Study. Mastre thesis, Universidade de Aveiro, Portugal, pp 49.
- Plecha, S., Silva, P.A., Vaz, N., Bertin, X., Oliveira, A., Fortunato, A.B. e Dias, J.M., 2010. Sensitivity analysis of a morphodynamic modelling system applied to a coastal lagoon inlet, *Ocean Dynamics*, 60/2: 275-284.
- Pritchard, D. W., 1967. What is an estuary: physical view point. p. 3–5 in: G. H. Lauf (ed.) *Estuaries*, A.A.A.S. Publ. No. 83, Washington, D.C.
- Ribeiro, R., Jorge, G., Pardal, P., Borges, A., Baptista, S., Tomás, L., Pinto, C., Santana, D., Barroso, R., 1994. Regularização da Ribeira de Aljezur – Estudo prévio. Ministério do Ambiente e Recursos Naturais, Instituto da Água. Hidroprojecto.
- Rodrigues, M., Oliveira, A., Queiroga, H., Guerreiro, M., Fortunato, A.B., Cravo, A., Freitas, M.C., Menaia, J., Dodkins, I., 2009. Dynamic modeling of dissolved oxygen in the Aljezur coastal stream (Portugal). ISEM 2009 Conference, Université Laval, Québec City, Canada.
- Rodrigues, M., Oliveira, A., Guerreiro, M., Fortunato, A.B., Menaia, J., David, L.M., Cravo, A., 2010. Modeling fecal contamination in the Aljezur coastal stream (Portugal). *Ocean Dynamics* pp. 44 (submitted)
- Soulsby, R., 1997. Dynamics of marine sands, a manual for practical applications. Thomas Telford, ISBN 0-7277-2584X, HR. Wallingford, England.

Turner, P. e A.M. Baptista, 1993. ACE/gredit User's Manual. Software for Semi-automatic Generation of Two-Dimensional Finite Element Grids. Center for Coastal and Land-Margin Research, Oregon Graduate Institute of Science & Technology.

Van De Graaff, J., Van Overeem, J., 1979. Evaluation of sediment transport formulae in coastal engineering practice. *Coastal Engineering* 3 (C), 1–32.

Work, P.A., Guan, J., Hayter, E.J., Elçi, S., 2001. Mesoscale model for morphologic change at tidal inlets. *Journal of Waterway, Port, Coastal and Ocean Engineering* 127 (5), 282–289.

Zhang, Y., Baptista, A.M., Myers, E.P., 2004. A cross-scale model for 3D baroclinic circulation in estuary-plume-shelf systems: I. Formulation and skill assessment. *Continental Shelf Research* 24 (18), 2187–2214.